Study of Lepton Number Conserving and Non-Conserving Processes Using GERDA Phase I Data

Sabine Hemmer

INFN Padova
Università degli Studi di Padova

Frascati, 24 June 2015

Outline

- Neutrinos and Double Beta Decay
- The GERDA experiment
- Monte Carlo Simulation of the GERDA Experiment
- Background Model for the GERDA Phase I Data
- $2\nu\beta\beta$ and $0\nu\beta\beta\chi(\chi)$ in GERDA Phase I
- $0\nu\beta\beta$ in GERDA Phase I

Unveil the nature of the neutrino

Majorana
$\nu = \bar{\nu}$

or

Dirac
$\nu \neq \bar{\nu}$

If $0\nu\beta\beta$ is observed:

Lepton number violation $\Delta L = 2$
Neutrino has a Majorana mass term
Sheds light on absolute neutrino mass scale
Sheds light on neutrino mass hierarchy

$2\nu\beta\beta$

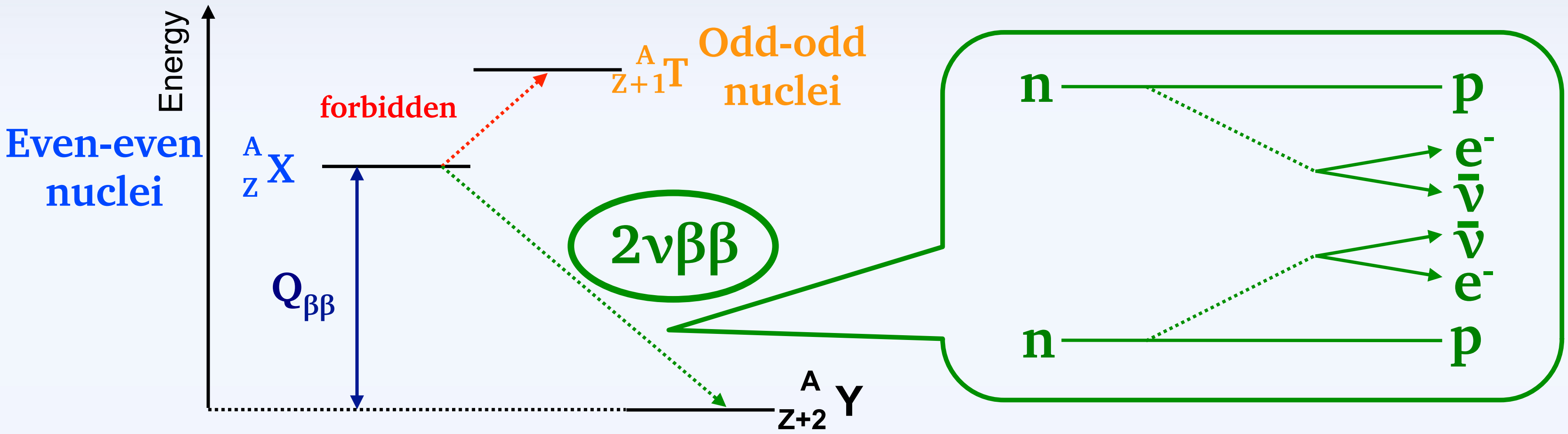

- allowed by SM
- $\Delta L=0$
- observed in many isotopes
- $T^{2\nu}_{1/2} \sim 10^{19}\text{-}10^{21}$yr
- $(T^{2\nu}_{1/2})^{-1} = G^{2\nu}(Q_{\beta\beta},Z) \cdot |M^{2\nu}|^2$

Phase space *nuclear matrix element*

$0\nu\beta\beta$

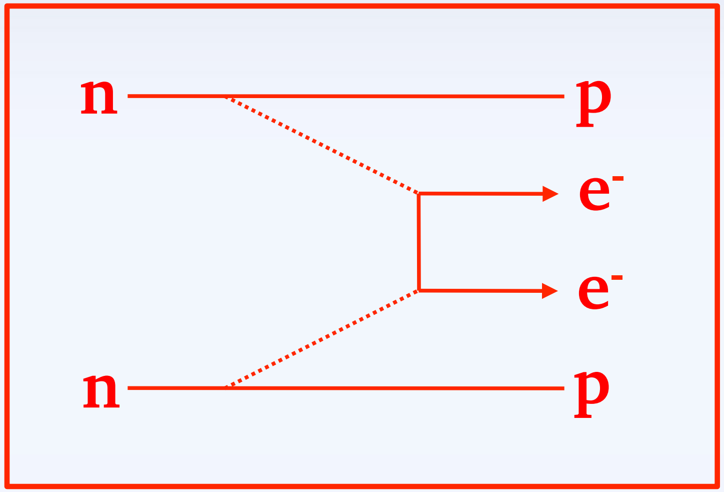

$|m_{\beta\beta}|$

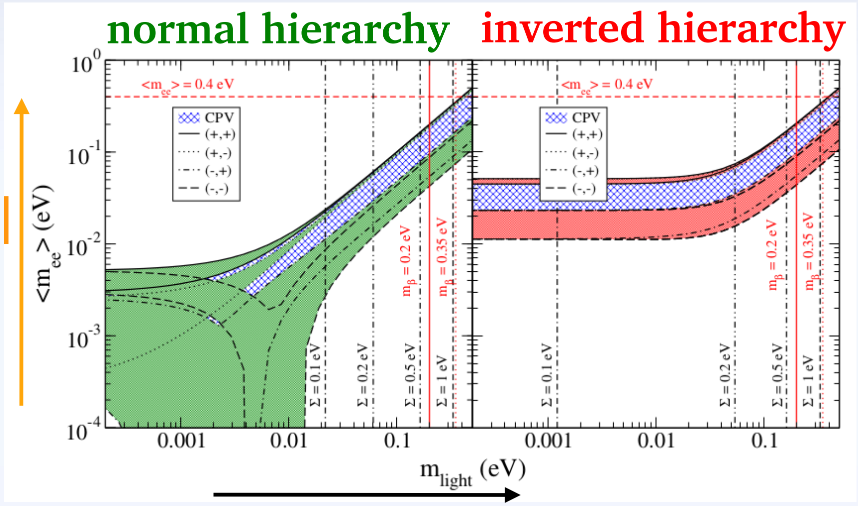

Lightest neutrino mass

- **Forbidden process in SM, needs Majorana neutrino**
- **$\Delta L=2$**
- $(T^{0\nu}_{1/2})^{-1} = G^{0\nu}(Q_{\beta\beta},Z)\cdot |M^{0\nu}|^2 \cdot \langle m_{\beta\beta}\rangle^2$ *

Phase space ($\sim Q_{\beta\beta}^5$)

nuclear matrix element

$\langle m_{\beta\beta}\rangle^2 = |\sum_i U_{ei}^2 m_i|^2$
Majorana neutrino mass

* Assuming exchange of light Majorana neutrino

0νββχ(χ)

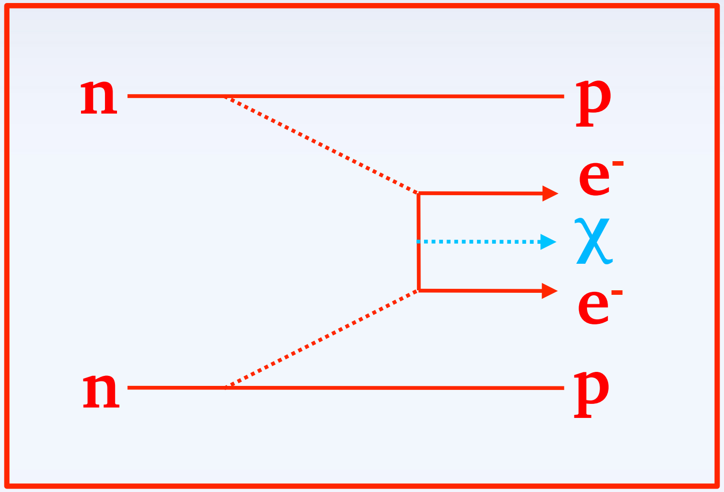

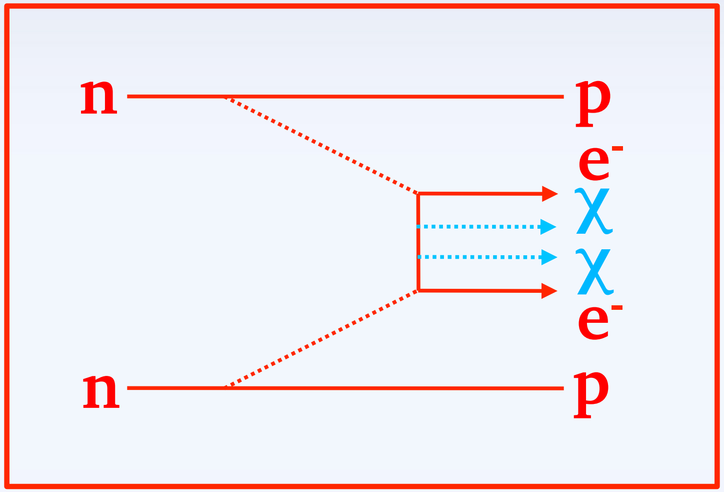

- Majoron χ: Additional particle emitted in 0νββ
- ΔL=2 or ΔL=0
- $(T^{0\nu\chi}_{1/2})^{-1} = |\langle g \rangle|^2 \cdot G^{0\nu\chi}(Q_{\beta\beta},Z) \cdot |M^{0\nu\chi}|^2$
- $(T^{0\nu\chi\chi}_{1/2})^{-1} = |\langle g \rangle|^4 \cdot G^{0\nu\chi\chi}(Q_{\beta\beta},Z) \cdot |M^{0\nu\chi\chi}|^2$

effective coupling constant

Phase space $\sim(Q_{\beta\beta}-E)^n$

nuclear matrix element

Spectral index n

0νββχ(χ)

Number of χ | Leptonic charge of χ | Spectral index

Lepton number violating / Lepton number conserving

Model	Mode	Goldstone boson	L	n	Matrix element
IB	χ	no	0	1	$M_F - M_{GT}$
IC	χ	yes	0	1	$M_F - M_{GT}$
ID	$\chi\chi$	no	0	3	$M_{F\omega^2} - M_{GT\omega^2}$
IE	$\chi\chi$	yes	0	3	$M_{F\omega^2} - M_{GT\omega^2}$
IF (bulk)	χ	bulk field	0	2	-
IIB	χ	no	-2	1	$M_F - M_{GT}$
IIC	χ	yes	-2	3	M_{CR}
IID	$\chi\chi$	no	-1	3	$M_{F\omega^2} - M_{GT\omega^2}$
IIE	$\chi\chi$	yes	-1	7	$M_{F\omega^2} - M_{GT\omega^2}$
IIF	χ	gauge boson	-2	3	M_{CR}

Experimental signatures

➡ **Measure combined electron energy spectrum E:**

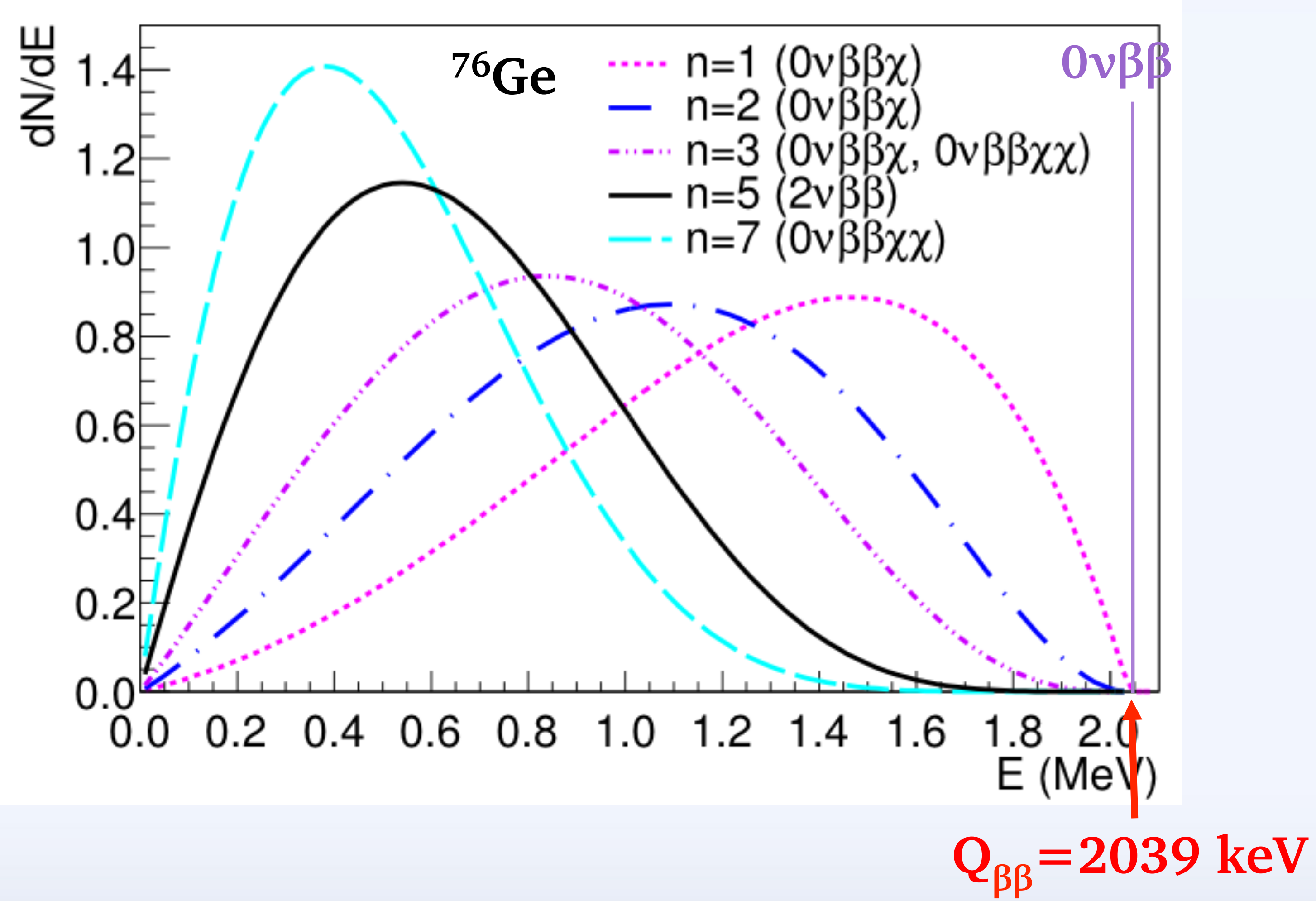

Previous measurements

Isotope	$T^{2\nu}_{1/2}$ (10^{19} yr)	$T^{0\nu}_{1/2}$ (yr) (90% C.L.)	$T^{0\nu\chi}_{1/2}$ (10^{21} yr) (90% C.L.) (n=1)
^{76}Ge	184^{+14}_{-10} [1]	$2.1\cdot10^{25}$ [2] $1.9\cdot10^{25}$ [3] $1.6\cdot10^{25}$ [4]	64 [3]
^{100}Mo	0.71 ± 0.04 [5]	$1.1\cdot10^{24}$ [6]	27 [7]
^{130}Te	68 ± 12 [5]	$4.0\cdot10^{24}$ [8]	16 [9]
^{136}Xe	216.5 ± 6.1 [10] 230 ± 12 [13]	$1.1\cdot10^{25}$ [11] $1.9\cdot10^{25}$ [14]	$1.2\cdot10^{3}$ [12] $2.6\cdot10^{3}$ [15]

Claim of signal for 0νββ:

$$T^{0\nu}_{1/2}\,(^{76}\mathrm{Ge}) = 1.19^{+0.37}_{-0.23}\cdot10^{25}\ \mathrm{yr}$$ [14]

[1] J. Phys. G: Nucl. Part. Phys. 40 (2013), 035110
[2] Phys. Rev. Lett. 111 (2013), 122503
[3] Eur. Phys. J. A12 (2001), 147-154
[4] Phys. Rev. D 65 (2002), 092007
[5] Phys. Atom. Nucl. 74 (2011), 603-613
[6] Phys. Atom. Nucl. 74 (2011), 312-317
[7] Nucl. Phys. A 765 (2006), 483-494
[8] arXiv:1504.02454
[9] Phys. Rev. Lett. 107 (2011), 062504
[10] Phys. Rev. C 89 (2014), 015502
[11] Nature 510 (2014), 229
[12] Phys. Rev. D 90 (2014), 092004
[13] Phys. Rev. C 86 (2012), 021601
[14] Phys. Rev. Lett. 110 (2013), 062502
[15] Phys. Lett. B 586 (2004), 198-212

Searching in ^{76}Ge

$$S \sim \epsilon \cdot f \cdot \sqrt{\frac{M \cdot t_{run}}{BI \cdot \Delta E}}$$

S: sensitivity
ε: efficiency
f: abundance of 0νββ isotope
M: detector mass

t_{run}: measurement time
BI: background index
ΔE: energy resolution at $Q_{\beta\beta}$

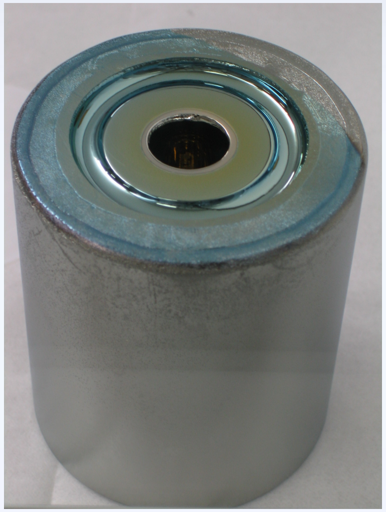

Germanium detector

Advantages of Germanium:

- High ε: Source = Detector
- Small instrinsic BI: High purity Ge
- Excellent ΔE: FWHM ~ (0.1-0.2)%
- Well-established technology

Disadvantages of Germanium:

- High external BI: $Q_{\beta\beta}$=2039keV
- Small f of ^{76}Ge: 7.8% → Enrichment needed!
- Limited sources of crystal & detector manufacturers
- Small $G^{0\nu}$ ($Q_{\beta\beta}$,Z)

Additional background reduction

Signal

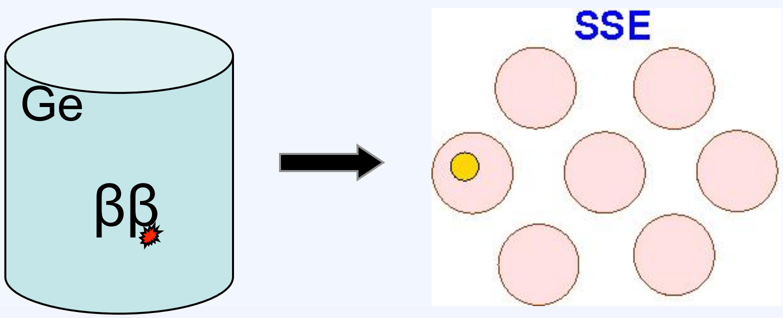

Point-like (single-site) energy deposition inside one HP-Ge diode (Range: ~ 1 mm)

Background

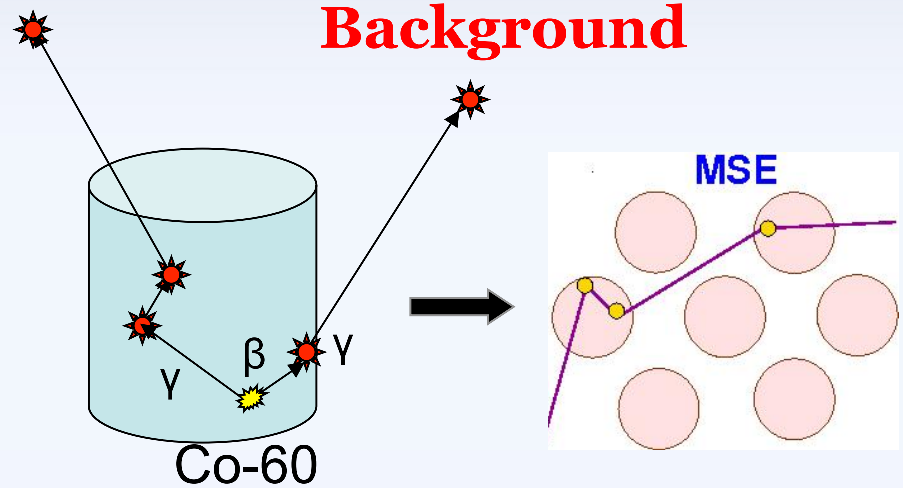

Multi-site energy deposition inside HP-Ge diode (Compton scattering)

Example of charge pulse

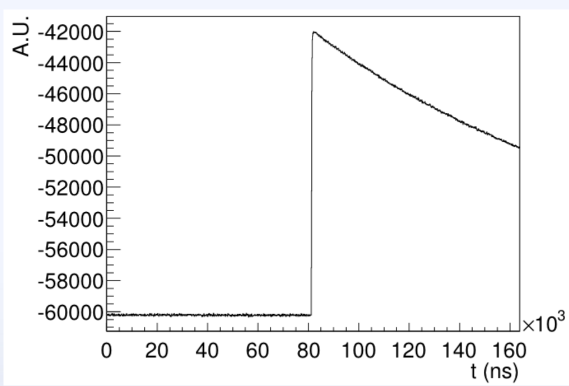

Signal analysis:

- anti-coincidence between detectors
- pulse shape analysis (PSA)

The GERDA experiment

- Situtated in LNGS underground laboratories (3500 m w.e. shielding)
- Graded shielding against ambient radiation
- Rigorous material selection, avoid exposure above ground for detectors

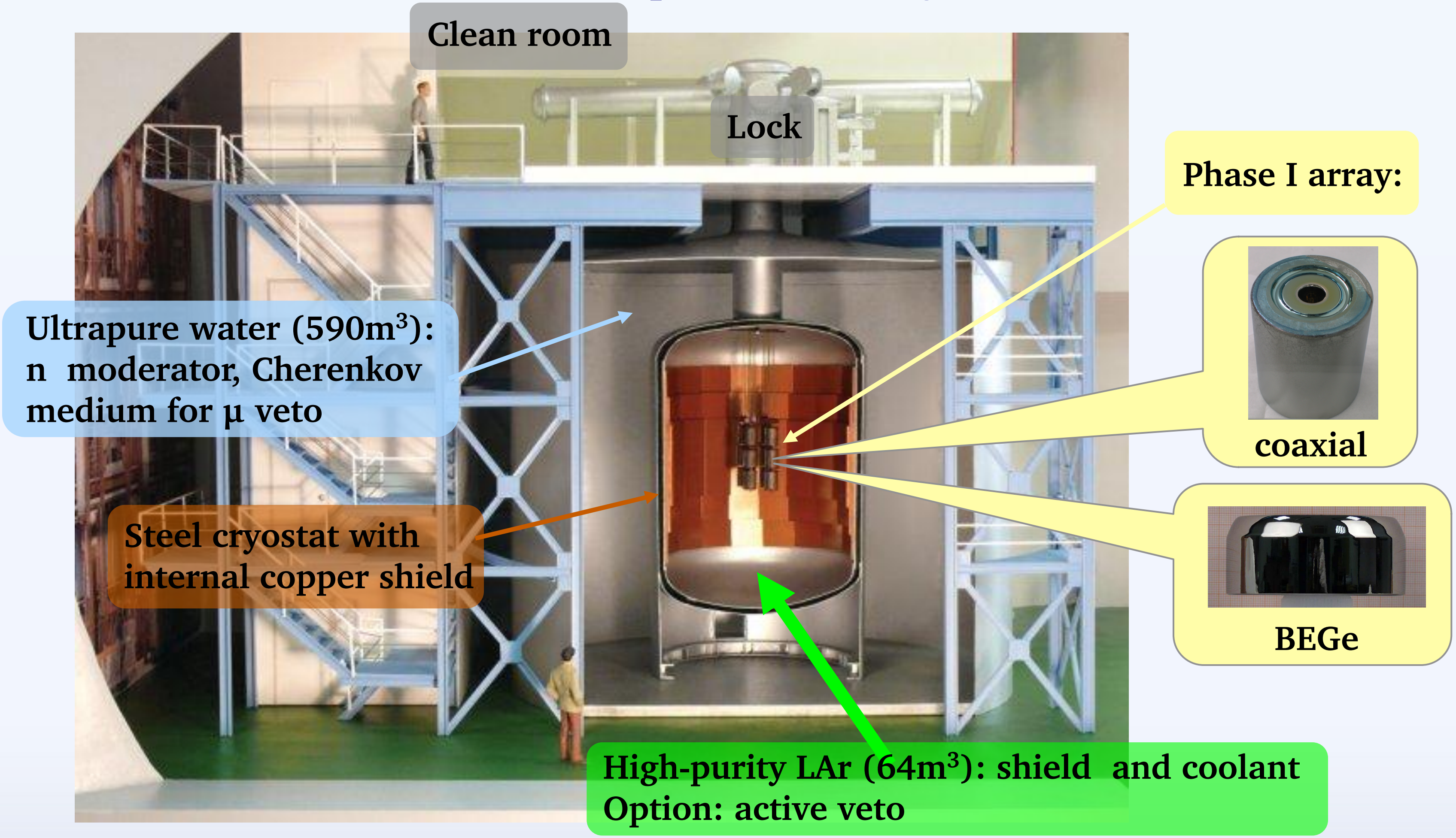

The GERDA experiment

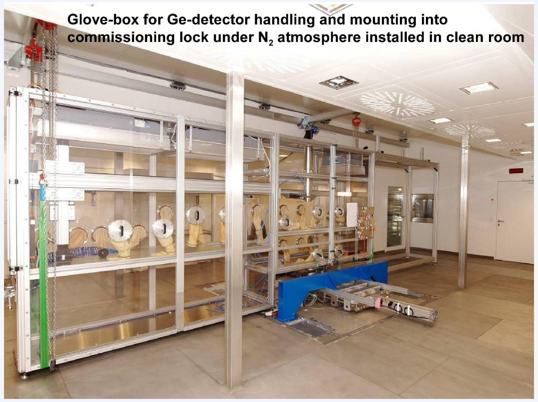
Glove-box for Ge-detector handling and mounting into commissioning lock under N_2 atmosphere installed in clean room

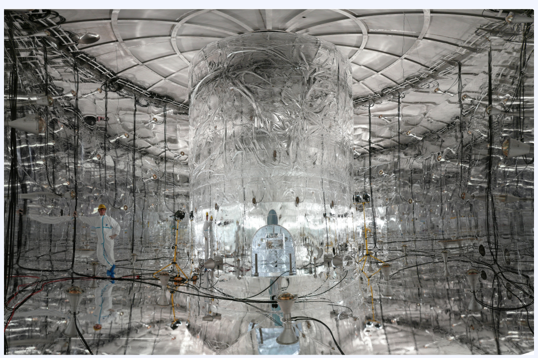

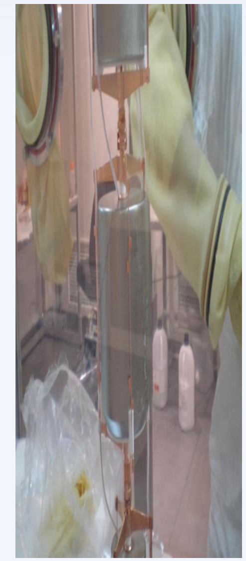

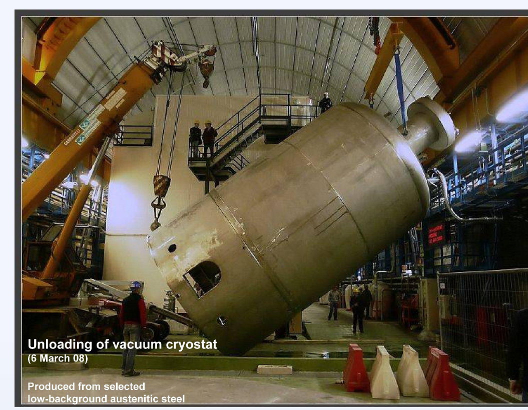
Unloading of vacuum cryostat
(6 March 08)
Produced from selected
low-background austenitic steel

GERDA Phase I data

Golden data set:
17.9 kg·yr with 6 coaxial detectors
FWHM at $Q_{\beta\beta}$=(4.83±0.19) keV

Silver data set:
1.3 kg·yr with 6 coaxial detectors
FWHM at $Q_{\beta\beta}$=(4.63±0.24) keV

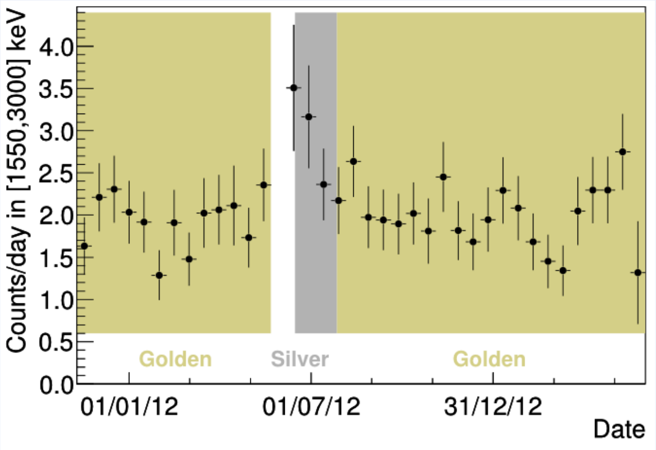

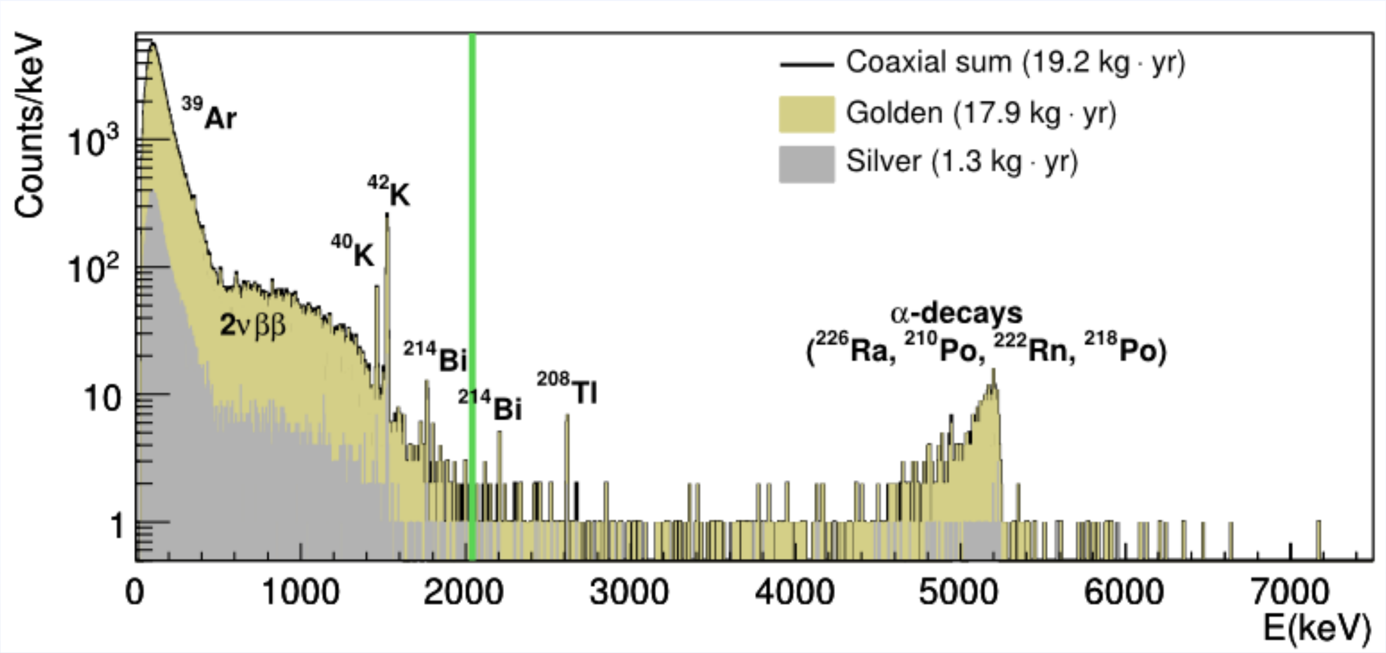

GERDA Phase I data

BEGe sum data set:
2.4 kg·yr with 4 BEGe detectors
FWHM at $Q_{\beta\beta}$=(3.24±0.17) keV

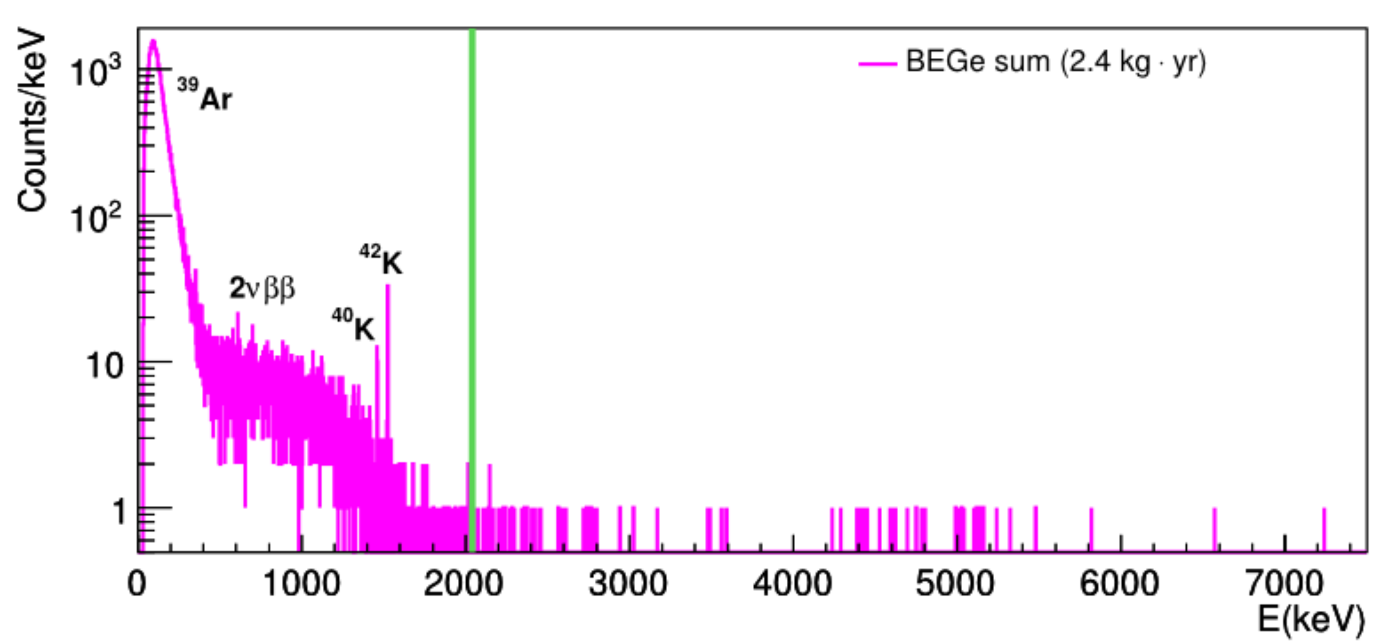

Background in GERDA Phase I data

Backgrounds assessed from

photon line intensities and **screening measurements**:

Isotope	Energy (keV)	Coaxial sum r_S cts/(kg·yr)	Golden r_S cts/(kg·yr)	Silver r_S cts/(kg·yr)	BEGe sum r_S cts/(kg·yr)
^{42}K	1524.7	60.6 [58.8,62.6]	59.6 [57.6,61.5]	75.1 [67.7,83.5]	46.6 [41.7,51.2]
^{40}K	1460.8	14.1 [12.9,15.2]	14.5 [13.2,15.6]	14.5 [13.2,15.6]	12.7 [9.6,15.9]
^{60}Co	1173.2	2.9 [1.3,4.4]	2.5 [0.9,4.0]	5.1 [0.8,9.9]	<8.6
	1332.5	<1.9	<1.8	5.2 [1.5,9.1]	<6.3
^{228}Ac	911.2	3.1 [1.1,4.9]	4.0 [1.8,5.9]	<8.9	<8.0
	969.0	6.7 [4.6,8.5]	5.6 [3.5,7.6]	19.7 [12.2,27.5]	<8.2
^{212}Bi	727.3	2.3 [0.5,4.1]	<4.7	17.8 [8.7,24.9]	<6.7
^{208}Tl	583.2	4.0 [1.9,6.2]	3.0 [1.0,5.0]	14.0 [5.9,21.8]	<11.0
	860.6	<3.1	<3.6	<11.9	<7.0
	2614.5	1.5 [1.1,1.7]	1.5 [1.1,1.7]	1.2 [0.2,2.4]	0.6 [0.1,1.3]
^{214}Pb	351.9	9.6 [4.3,14.1]	10.1 [5.0,15.2]	<34.8	13.5 [5.6,22.7]
^{214}Bi	609.3	8.1 [5.6,10.3]	8.6 [5.9,10.8]	<16.1	12.0 [6.7,18.2]
	768.4	4.3 [2.1,6.3]	3.6 [1.4,5.5]	16.9 [8.1,23.9]	6.5 [1.6,10.7]
	1120.3	<2.9	<3.1	<8.9	6.7 [2.5,10.7]
	1238.1	<2.8	<2.8	<10.7	<6.6
	1764.5	3.2 [2.7,3.7]	3.3 [2.7,3.7]	2.2 [0.2,4.0]	<2.5
	2204.2	0.9 [0.6,1.2]	0.9 [0.6,1.2]	<3.3	1.0 [0.3,1.8]
^{137}Cs	661.7	<4.6	<5.0	<14.7	7.0 [2.3,11.8]
e^+e^- & ^{208}Tl	511.0	10.4 [7.8,12.8]	10.6 [7.9,13.1]	<20.0	16.5 [10.4,21.9]

Component	units	^{40}K	$^{214}Bi/^{226}Ra$	^{228}Th	^{60}Co	^{222}Rn	*BI*
Close sources: up to 2 cm from detectors							
Copper det. support	µBq/det	<7	<1.3	<1.5			<0.2
PTFE det. support	µBq/det	6.0 (11)	0.25 (9)	0.31 (14)			0.1
PTFE in array	µBq/det	6.5 (16)	0.9 (2)				0.1
minishroud	µBq/det		22 (7)				2.8
Li salt (n^+-contact)	mBq/kg		17 (5)				≈ 0.003
Medium distant sources: 2 cm to 50 cm from detectors							
CC2 preamps	µBq/det	600 (100)	95 (9)	50 (8)			0.8
cables and suspension	mBq/m	1.40 (25)	0.4 (2)	0.9 (2)	76 (16)		0.2
Distant sources: further than 50 cm from detectors							
cryostat	mBq					54.7 (35)	<0.7
copper of cryostat	mBq	<784	264 (80)	216 (80)	288 (72)		<0.05
steel of cryostat	kBq	<72	<30	<30	475		
lock system	mBq					2.4 (3)	<0.03
^{228}Th calib. source	kBq		20				<1.0

Monte Carlo Simulation

- Detailed description of geometry in GEANT4 based MaGe framework

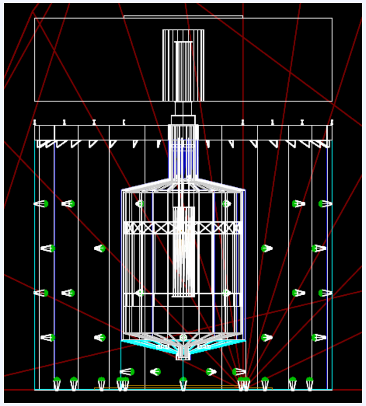

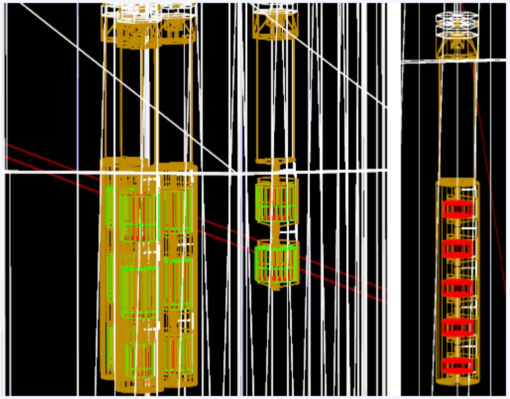

- Account for energy resolution and data selection cuts

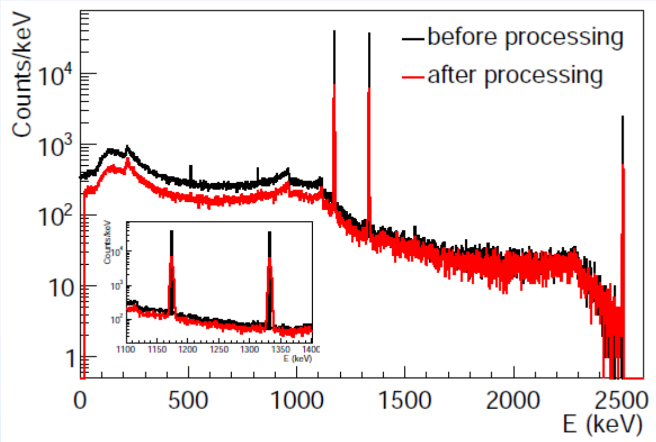

Monte Carlo Simulation

Simulate all relevant contributions to the energy spectra

- ^{76}Ge ($2\nu\beta\beta$ and $0\nu\beta\beta\chi(\chi)$)
  intrinsic
- ^{214}Bi sub-chain
  holders, shroud, p^+-contact, minishrouds, n^+-contact, in LAr
- ^{228}Ac
  holders, shroud
- ^{228}Th sub-chain
  holders, shroud, heat exchanger
- ^{60}Co
  holders, intrinsic
- ^{68}Ga (only for BEGe data set)
  intrinsic
- ^{40}K
  holders
- ^{42}K
  in LAr, p^+-contact, n^+-contact
- α-decays from ^{226}Ra sub-chain and ^{210}Po
  p^+-contact, LAr close to p^+-contact

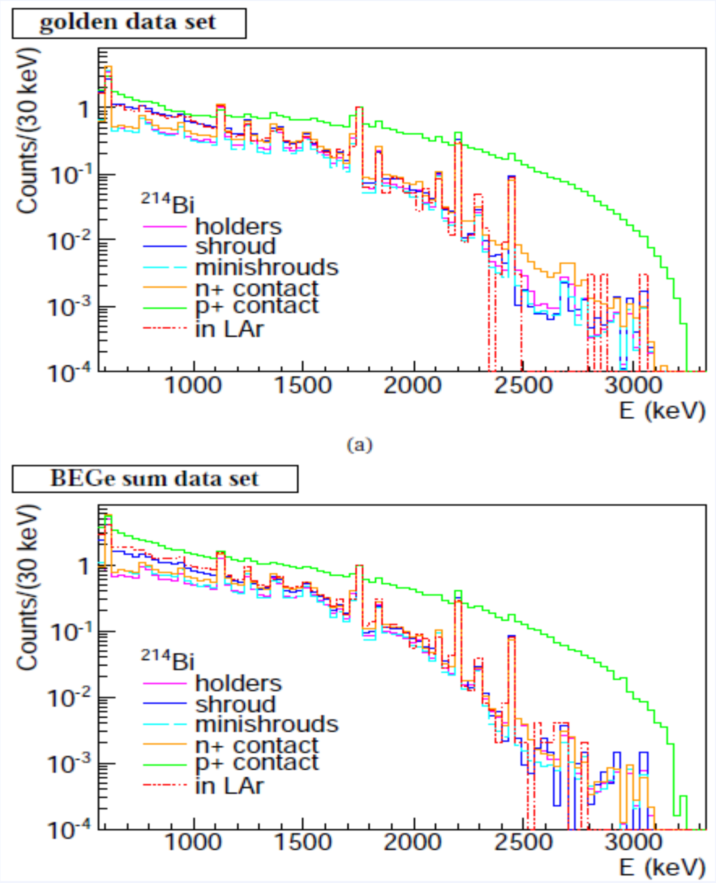

Background model

Binned maximum likelihood approach using BAT framework
→ posterior probability distribution for model λ given data spectrum n:

$$P(\boldsymbol{\lambda}|\mathbf{n}) = \frac{P(\mathbf{n}|\boldsymbol{\lambda})P_0(\boldsymbol{\lambda})}{\int P(\mathbf{n}|\boldsymbol{\lambda})P_0(\boldsymbol{\lambda})d\boldsymbol{\lambda}}$$

derived with Bayes' theorem from likelihood

$$P(\mathbf{n}|\boldsymbol{\lambda}) = \prod_i P(n_i|\lambda_i) = \prod_i \frac{e^{-\lambda_i}\lambda_i^{n_i}}{n_i!}$$

$\lambda_i = \sum_c \lambda_i^c$: **sum of contributions from single components, c, in i-th bin**

n_i: **number of events in i-th bin of data spectrum**

➡ **one parameter for each model contribution!**

➡ **best-fit results and marginalized results!**

Background model

- Build separate models for golden and BEGe sum data set
- Alpha models:
  - fit to high energy region with alpha components → [3500; 7500] keV in 50 keV bins
- Full background models:
  - fit to full energy range → [570; 7500] keV in 30 keV bins
  - alpha model contributes as one component
  - ^{214}Bi on p$^+$-surface, intrinsic ^{60}Co and ^{68}Ga, ^{214}Bi sub-chain on holders and shroud, ^{228}Th sub-chain on holders and shroud informative prior based on prior knowledge
  - region between 2019 keV and 2059 keV blinded

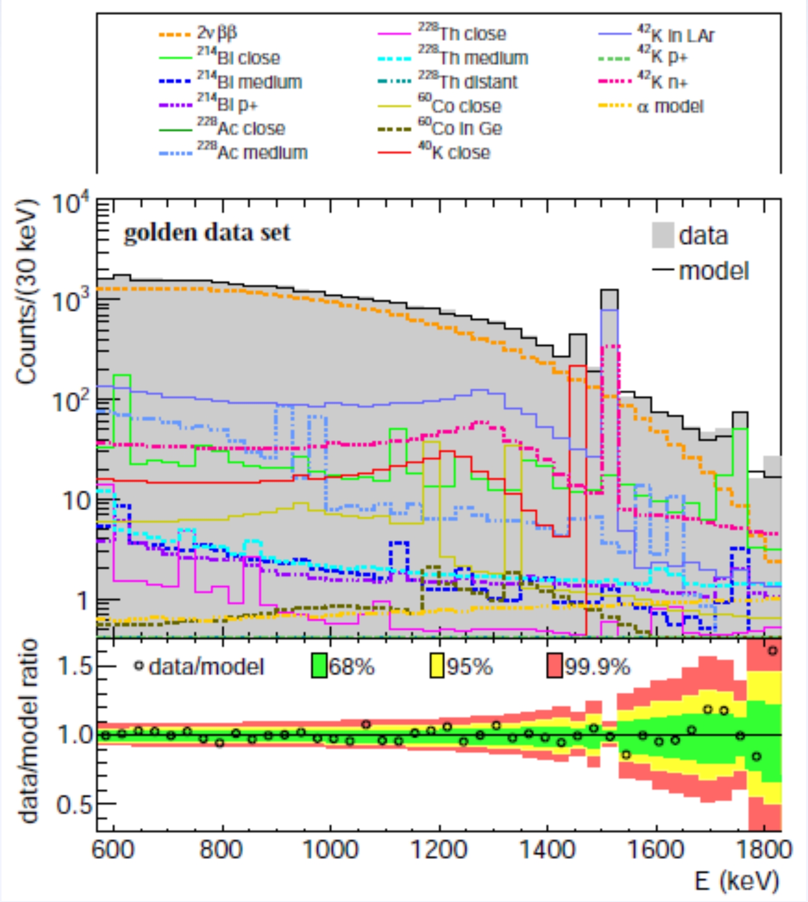

Background model around $Q_{\beta\beta}$

BI (10^{-3} cts/(keV·kg·yr)):

Model: 21.0 [19.8,22.2]
Data: $18.5^{+2.3}_{-2.2}$

Model: 40.6 [36.5,45.2]
Data: $41.3^{+10.4}_{-8.4}$

Golden data set

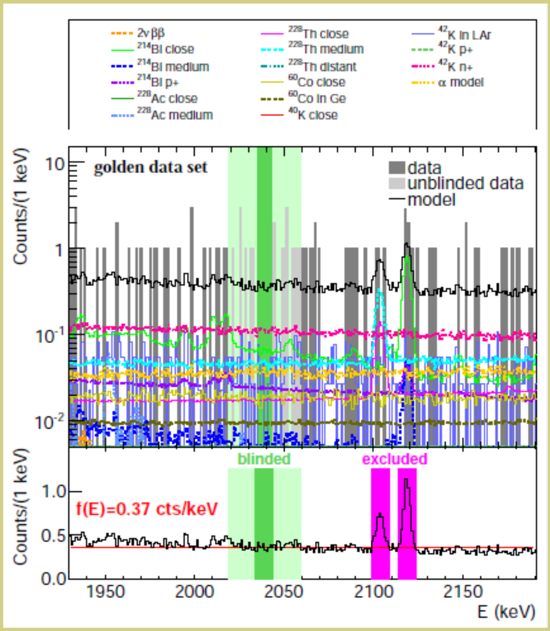

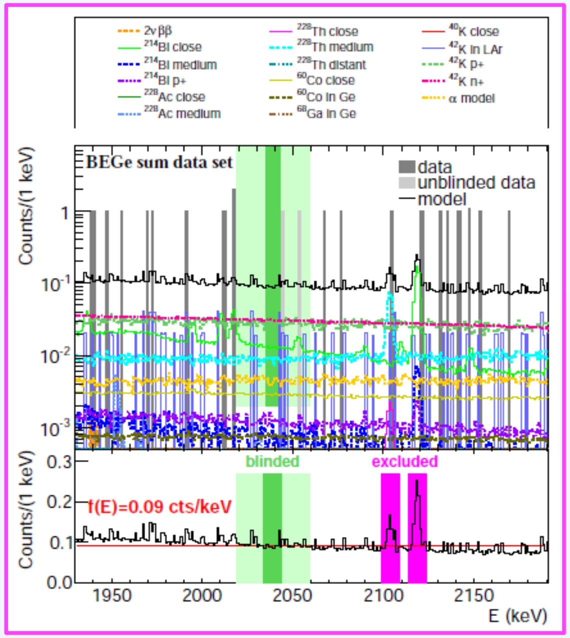

BEGe sum data set

- BI in [1930; 2190] keV can be approximated as flat
- Dominant contributions:
  ^{214}Bi and ^{228}Th sub-chain decays, ^{42}K decays, and α-decays
- BI predictions around $Q_{\beta\beta}$ stable for variations within uncertainties of priors, active volume fractions, enrichment fractions, as well as for different source positions and binning

2νββ - Analysis

Measure $T^{2\nu}_{1/2}$ → combine information from golden and BEGe sum data set:

$$P(\mathbf{n}^{gold}, \mathbf{n}^{BEGe} | \boldsymbol{\lambda}^{gold}, \boldsymbol{\lambda}^{BEGe}) = \prod_i P(n_i^{gold} | \lambda_i^{gold}) \cdot \prod_j P(n_j^{BEGe} | \lambda_j^{BEGe})$$

→ $T^{2\nu}_{1/2}$ common parameter for both data sets

$$T^{2\nu}_{1/2} = 1.96\ [1.93, 1.99] \cdot 10^{21}\ \text{yr}$$

(systematic uncertainty not accounted for)

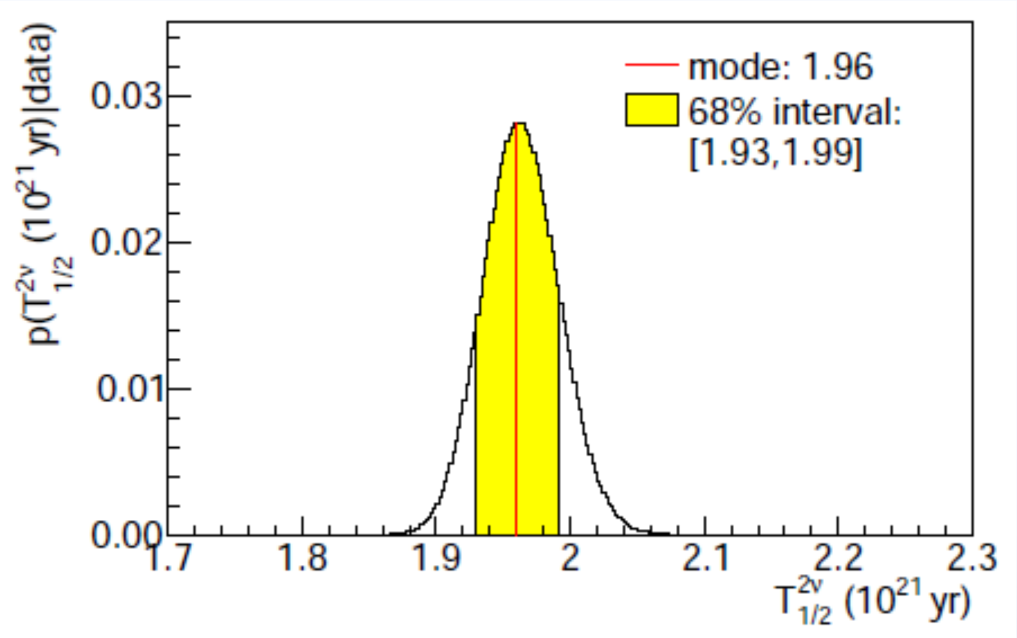

2νββ - Analysis

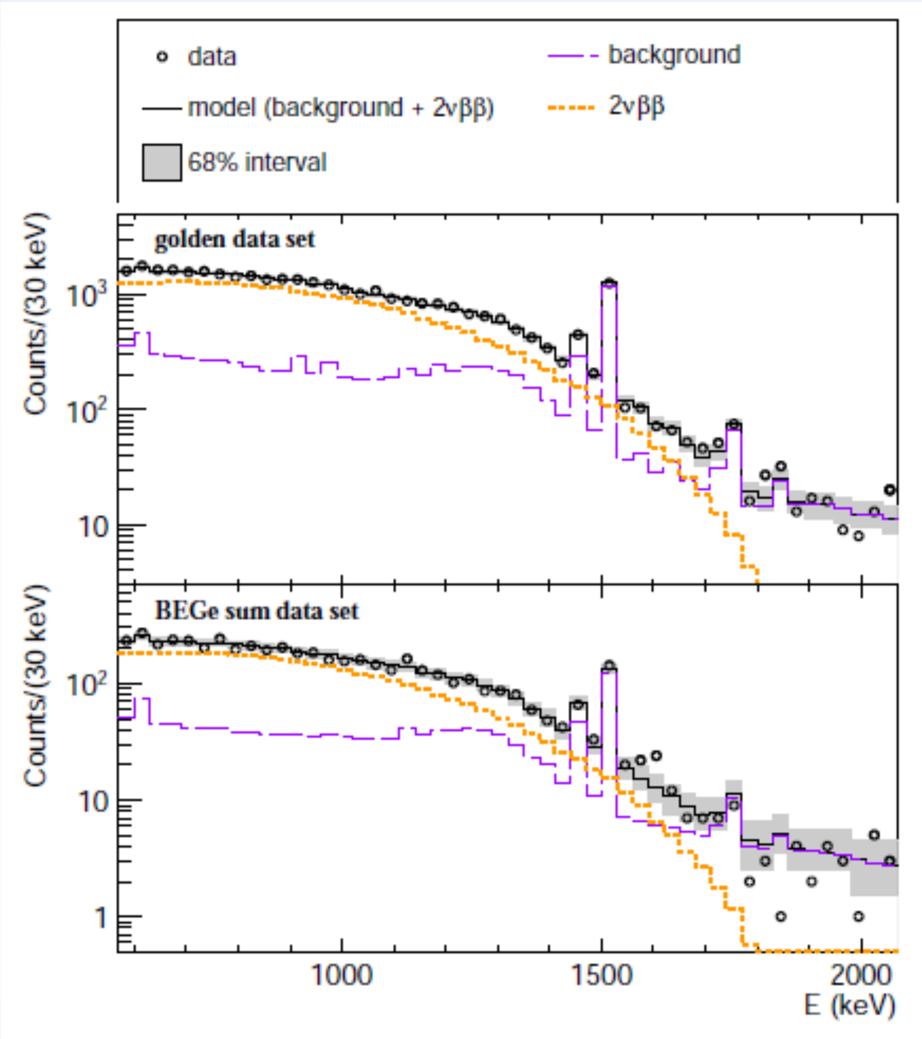

Signal to background:
3:1

Golden:
Data: 35868 events
Best-fit model: 35902.3 events

BEGe sum:
Data: 5035 events
Best-fit model BEGe sum: 5062.1 events

0νββχ(χ) - Analysis

Add also contributions from Majoron mode (n=1, 2, 3, or 7) to model

→ $1/T^{0\nu\chi(\chi)}_{1/2}$ common parameter for both data sets

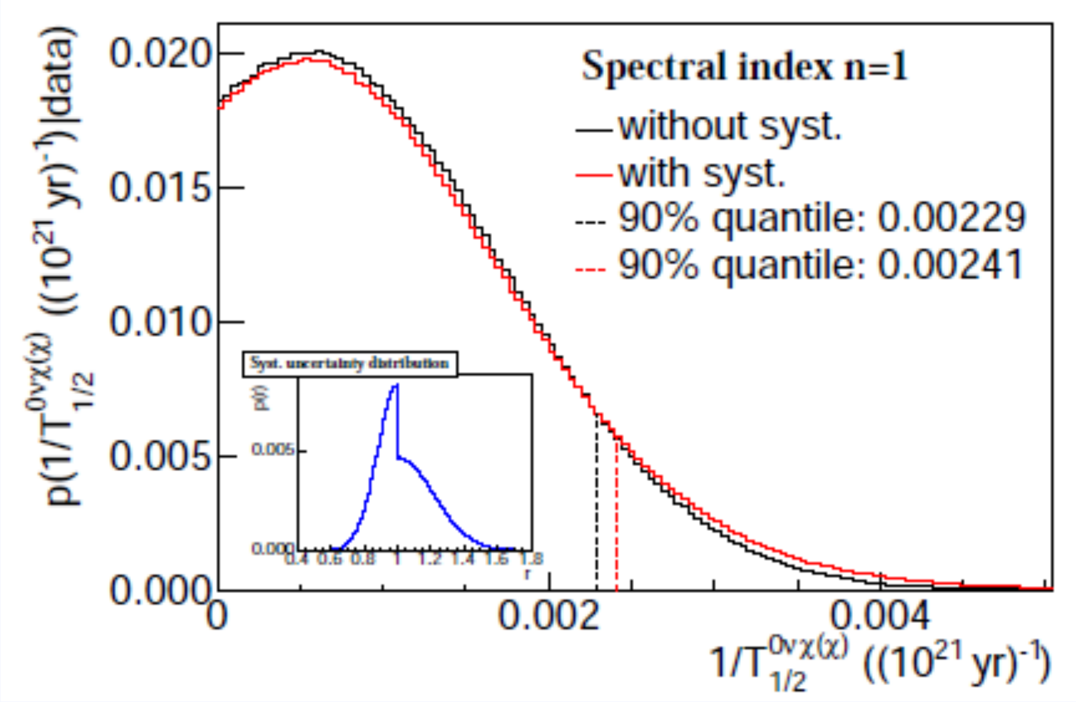

$T^{0\nu\chi(\chi)}_{1/2}$ (90% quantile)	
n=1	$> 4.36\cdot10^{23}$ yr
n=2	$> 1.91\cdot10^{23}$ yr
n=3	$> 0.94\cdot10^{23}$ yr
n=7	$> 0.35\cdot10^{23}$ yr

(systematic uncertainty not accounted for)

0νββχ(χ) - Analysis

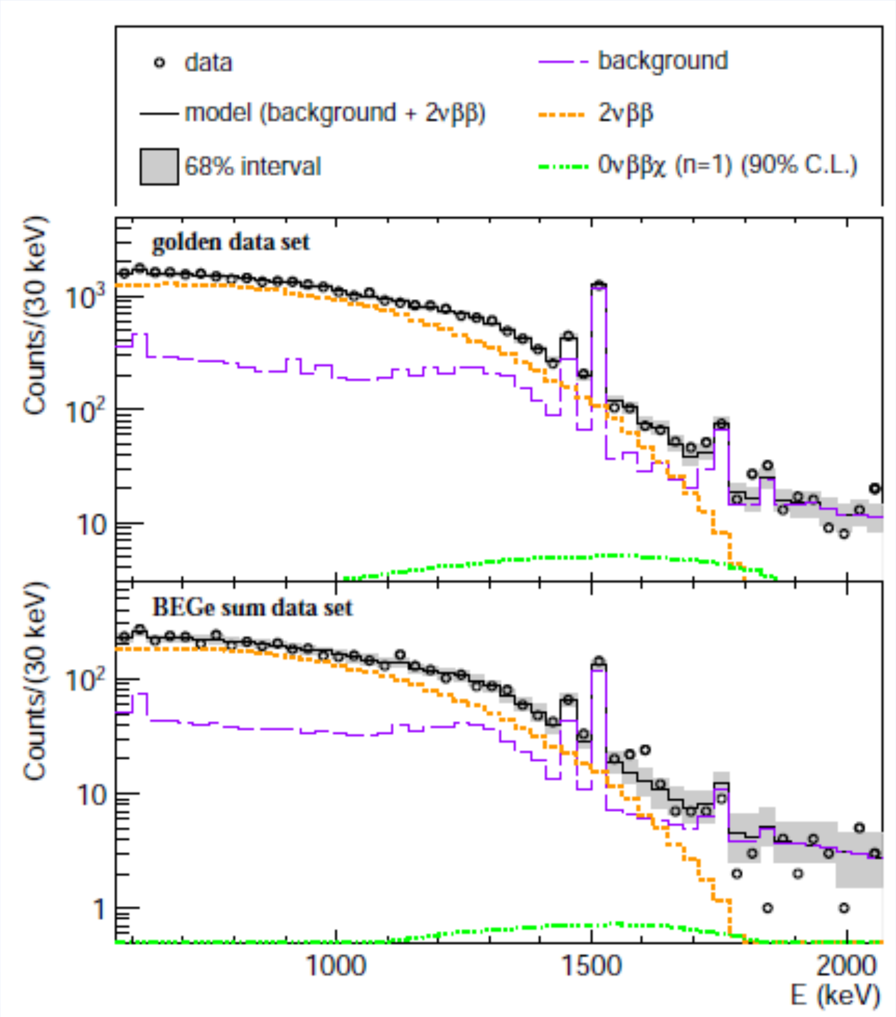

- For all spectral modes good agreement of best-fit model with data
- Result for $T^{2\nu}_{1/2}$ in all cases in agreement with previous result

Systematic uncertaintes

Systematic uncertainties estimated by cross-checks changing conditions in fit or input parameters (case n=1 chosen as representative)

Item	Uncertainty on $T^{2\nu}_{1/2}$ (%)	Uncertainty on $1/T^{0\nu\chi(\chi)}_{1/2}$ (% on 90% quantile)
Screening results	–	$^{+0.5}_{-1.3}$
Binning	±0.5	+16.1
Active volume fraction	±5.6	$^{+5.7}_{-8.0}$
Enrichment fraction	±2.0	±1.7
Source positions	–	$^{+12.6}_{-8.3}$
Transition layer	±0.5	±0.5
Total fit model	**±6.0**	$^{+21.3}_{-11.7}$
MC geometry	±1.0	±1.0
MC tracking	±2.0	±2.0
Total MC simulation	**±2.2**	**±2.2**
Data acquisition and selection	±0.5	±0.5
Total systematic uncertainty	**±6.4**	$^{+21.4}_{-12.0}$

Add individual contributions in quadrature

For limits on $1/T^{0\nu\chi}_{1/2}$: Fold systematic uncertainty in posterior distribution

$2\nu\beta\beta$ – Final result

$$T_{1/2}^{2\nu} = (1.96 \pm 0.03_{fit} \pm 0.13_{syst}) \cdot 10^{21}\ yr = (1.96 \pm 0.13) \cdot 10^{21}\ yr$$

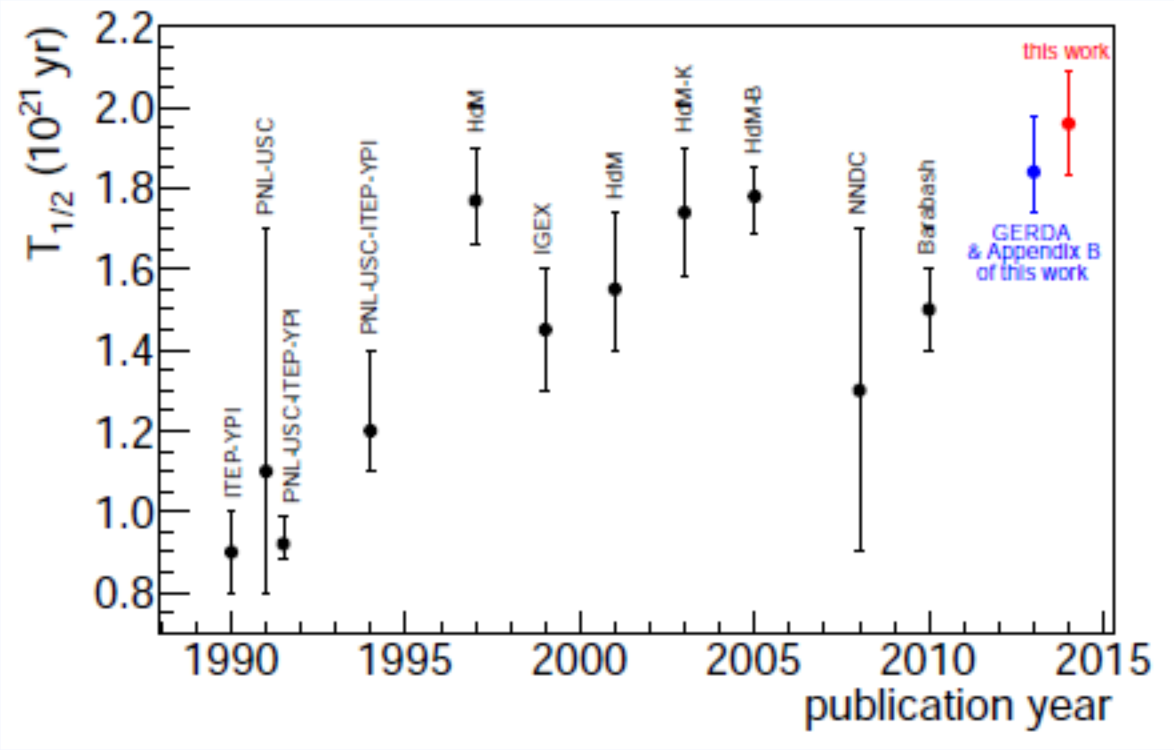

Good agreement with previous measurement using GERDA data

$0\nu\beta\beta\chi(\chi)$ – Final results

Model	n	Mode	Goldstone boson	L	$T^{0\nu\chi}_{1/2}$ $[10^{23}\mathrm{yr}]$	$\mathcal{M}^{0\nu\chi}$	$G^{0\nu\chi}$ $[\mathrm{yr}^{-1}]$	$\langle g \rangle$
IB	1	χ	no	0	> 4.2	$(2.30 - 5.82)$	$5.86 \cdot 10^{-17}$	$< (3.4 - 8.7) \cdot 10^{-5}$
IC	1	χ	yes	0	> 4.2	$(2.30 - 5.82)$	$5.86 \cdot 10^{-17}$	$< (3.4 - 8.7) \cdot 10^{-5}$
ID	3	$\chi\chi$	no	0	> 0.8	$10^{-3\pm1}$	$6.32 \cdot 10^{-19}$	$< 2.1^{+4.5}_{-1.4}$
IE	3	$\chi\chi$	yes	0	> 0.8	$10^{-3\pm1}$	$6.32 \cdot 10^{-19}$	$< 2.1^{+4.5}_{1.4}$
IF	2	χ	bulk field	0	> 1.8	–	–	–
IIB	1	χ	no	-2	> 4.2	$(2.30 - 5.82)$	$5.86 \cdot 10^{-17}$	$< (3.4 - 8.7) \cdot 10^{-5}$
IIC	3	χ	yes	-2	> 0.8	0.16	$2.07 \cdot 10^{-19}$	$< 4.7 \cdot 10^{-2}$
IID	3	$\chi\chi$	no	-1	> 0.8	$10^{-3\pm1}$	$6.32 \cdot 10^{-19}$	$< 2.1^{+4.5}_{-1.4}$
IIE	7	$\chi\chi$	yes	-1	> 0.3	$10^{-3\pm1}$	$1.21 \cdot 10^{-18}$	$< 2.2^{+4.9}_{-1.4}$
IIF	3	χ	gauge boson	-2	> 0.8	0.16	$2.07 \cdot 10^{-19}$	$< 4.7 \cdot 10^{-2}$

Most stringent limits obtained to date for Majoron accompanied decay of ^{76}Ge

Blinded analysis

Use Pulse Shape Analysis (PSA):
Event selection based on charge and current pulse characteristics

Combine information from golden, silver, and BEGe sum data set:

$$\text{Total likelihood } L = L_{golden} \cdot L_{silver} \cdot L_{BEGe}$$

Fit function: constant + gaussian peak centered at $Q_{\beta\beta}$
➡ 4 parameters (background of three data sets and $T^{0\nu}_{1/2}$)

Systematic uncertainties folded in with Monte Carlo approach:
Probability distribution for each source of uncertainty

- Detection efficiency ($\langle\varepsilon\rangle = \langle f_{76} \cdot f_{act} \cdot f_{FEP} \rangle$)
- Energy resolution
- Signal acceptance after PSA
- Position of the signal peak

$0\nu\beta\beta$ – Final Results

Expectation in ROI (after PSA): 2.0±0.3 events
Observation in ROI (after PSA): 3 events (none in ±σ around $Q_{\beta\beta}$)

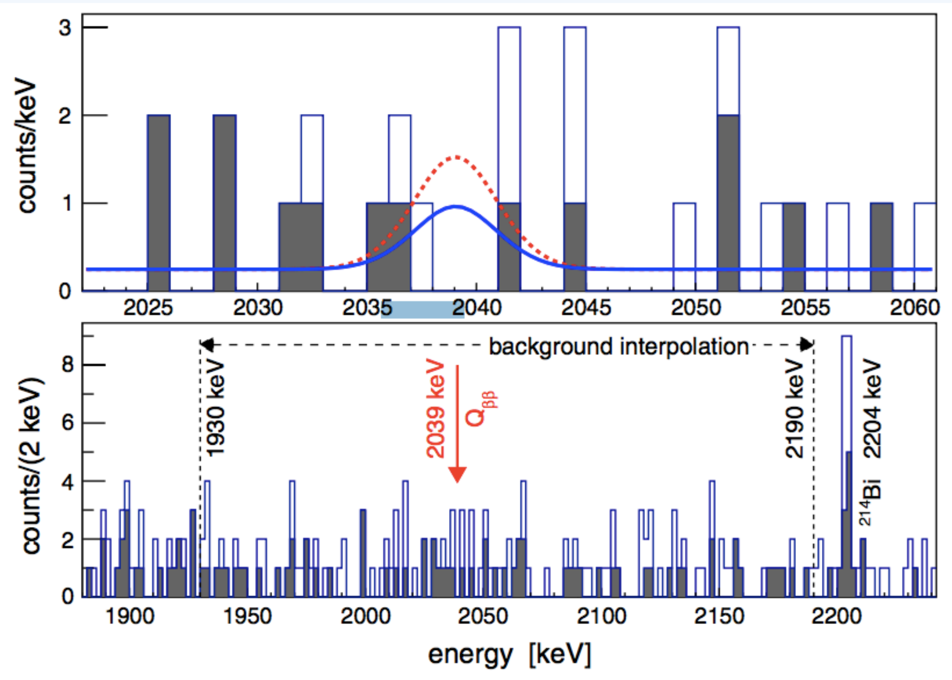

Final GERDA result *:
$T^{0\nu}_{1/2} > 2.1 \cdot 10^{25}$ yr (90% C.L.)

Combine with information from energy spectra of HDM and IGEX:
$T^{0\nu}_{1/2} > 3.0 \cdot 10^{25}$ yr (90% C.L.)

Assuming exchange of light Majorana neutrino as dominating mechanism for $0\nu\beta\beta$:
$<m_{\beta\beta}> < (0.2\text{-}0.4)$ eV

*frequentist approach, with Bayesian approach: $T^{0\nu}_{1/2} > 1.9 \cdot 10^{25}$ yr (90% C.I.)

Signal claim of $T^{0\nu}_{1/2} = 1.19^{+0.37}_{-0.23} \cdot 10^{25}$ yr [1] not supported

[1] H.V. Klapdor-Kleingrothaus et al., Phys. Lett. B 586 (2004) 198-212

Conclusions

Analysis of GERDA Phase I data comprising:

- Description of all relevant background sources with MC simulation
- Development of complete background model
- Measurement of half-life of $2\nu\beta\beta$ of ^{76}Ge with unprecedented precision: $T^{2\nu}_{1/2}=(1.96\pm0.13)\cdot10^{21}$ yr
- Search for $0\nu\beta\beta\chi(\chi)$ modes of ^{76}Ge leading to improved lower limits for all four modes
- Search for $0\nu\beta\beta$ of ^{76}Ge resulting in $T^{0\nu}_{1/2}>2.1\cdot10^{25}$ yr

Additional material

Previous measurements and claim

Previous 0νββ experiments

	HdM	IGEX
Location	LNGS	Homestake, Baksan, Canfranc
Exposure [kg·yr]	71.1	8.8
Bg [cts/(keV·kg·yr)]	≥ 0.11	0.17
$T_{1/2}$ limit (90% CL) [yr]	$1.9 \cdot 10^{25}$ [1]	$1.6 \cdot 10^{25}$ [2]

[1] *Eur. Phys. J. A12, 147-154 (2001)*
[2] *Phys. Rev. D 65, 092007 (2002)*

Claim of signal from part of HdM:

$T_{1/2}\,(^{76}Ge) = 1.19^{+0.37}_{-0.23} \cdot 10^{25}$ yr *Phys. Lett. B 586, 198-212 (2004)*

HdM claim

Data acquisition and analysis of the ^{76}Ge double beta experiment in Gran Sasso 1990–2003

H.V. Klapdor-Kleingrothaus*[,1], A. Dietz, I.V. Krivosheina[2], O. Chkvorets

Phys. Lett. B 586, 198-212 (2004)

BI 0.11 cts / (keV·kg·yr)

28.75 ± 6.87 events (bgd:~60)

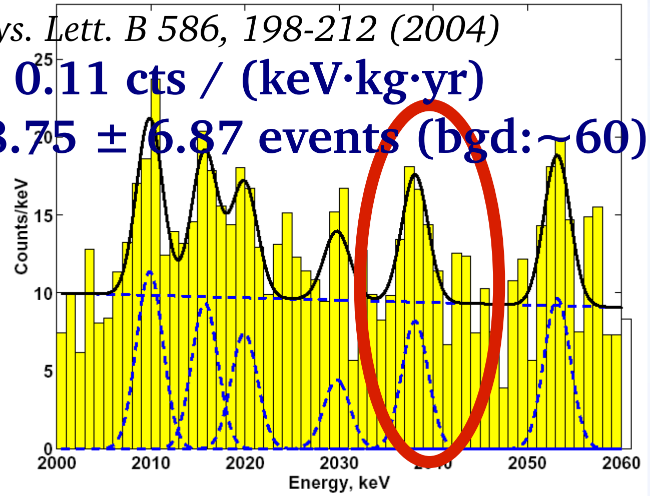

Fig. 17. The total sum spectrum of all five detectors (in total 10.96 kg enriched in ^{76}Ge), for the period November 1990–May 2003 (71.7 kg year) in the range 2000–2060 keV and its fit (see Section 3.2).

Comparison: IGEX

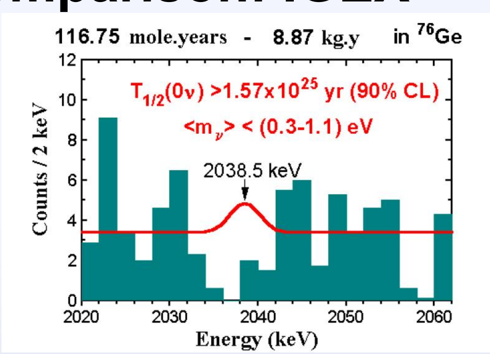

- Nov 1990 - May 2003
- 71.7 kg·yr
- 4.2σ/6σ evidence for 0νββ

- $(0.69 – 4.18)\cdot 10^{25}$ yr (3σ)
  Best fit: $1.19\cdot 10^{25}$ yr

Phys. Lett. B 586, 198-212 (2004)

$2.23^{+0.44}_{-0.31}\cdot 10^{25}$ yr

Mod. Phys. Lett. A 21, 1547-1566 (2006)

Criticism in *Ann. Phys. 525, 269-280 (2013)*

- $m_{\beta\beta}$ = (0.24-0.58) eV (best fit 0.44 eV) / 0.32±0.03 eV

Note: statistical significance depends on background model!

Refusal of signal claim

Assuming $T^{0\nu}_{1/2}=1.19^{+0.37}_{-0.23}\cdot 10^{25}$ yr: expect **5.9±1.4 signal events** in ROI

Expectation from background (after PSA): **2.0±0.3 events** in ROI

Observation: **3 events**

From analysis:

BF<<1 for both frequentist and Bayesian approaches

Best fit value: $N^{0\nu}=0$ for both approaches

$P(N^{0\nu}=0\,|\,T^{0\nu}_{1/2}=1.19\cdot 10^{25}$ yr$)=0.01$ for frequentist approach

➡ **Claim of observation of 0νββ not supported by GERDA Phase I data**

BI definition

Definition of BI

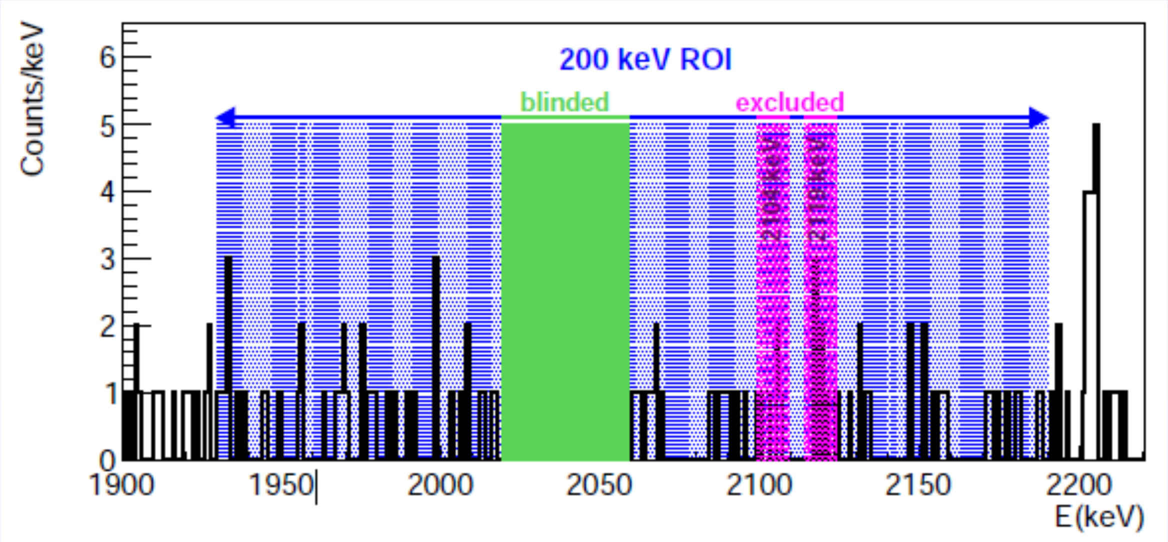

BI (10^{-3} cts/(keV·kg·yr)) after partial unblinding:

	Before PSA	After PSA
Golden:	$18.5^{+2.3}_{-2.2}$	$10.9^{+1.9}_{-1.6}$
Silver:	$63.4^{+18.0}_{-14.3}$	$30.1^{+13.7}_{-9.8}$
BEGe sum:	$41.3^{+10.4}_{-8.4}$	$5.4^{+5.2}_{-2.9}$

Pulse Shape Analysis

Pulse shape analysis – BEGe detectors

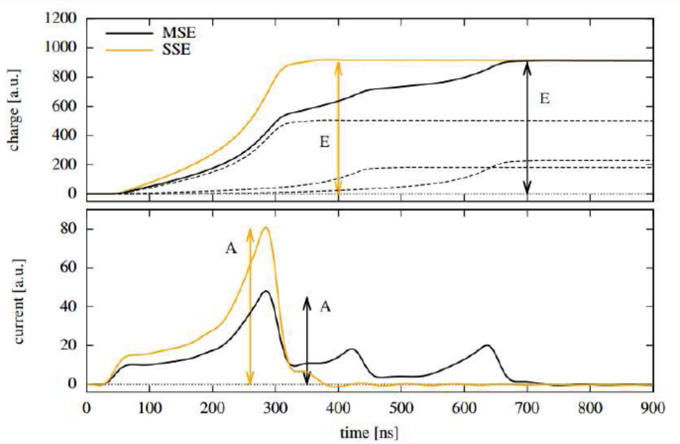

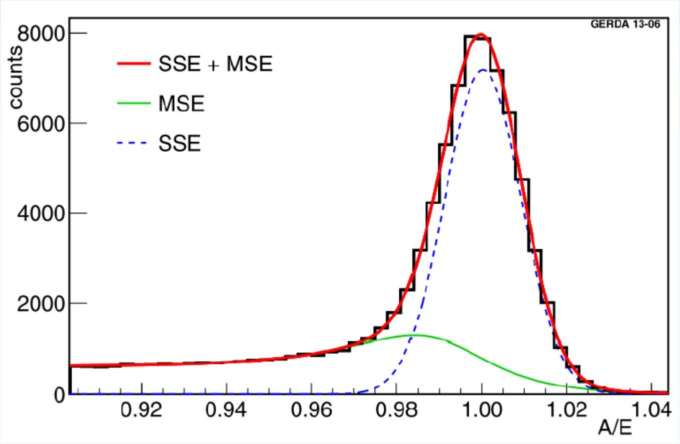

Cut based on A/E → keep events with $2\sigma_{A/E} < A/E < 4\sigma_{A/E}$
(tuned using DEP, compton continuum and $2\nu\beta\beta$ events)

$\varepsilon_{PSA} = 0.92 \pm 0.02$ for SSE

BI (10^{-3} cts/(keV·kg·yr)) after partial unblinding:

	Before PSA	After PSA
BEGe sum:	$41.3^{+10.4}_{-8.4}$	$5.4^{+5.2}_{-2.9}$

In ROI: 1 event detected → rejected by PSA

Pulse shape analysis – coaxial detectors

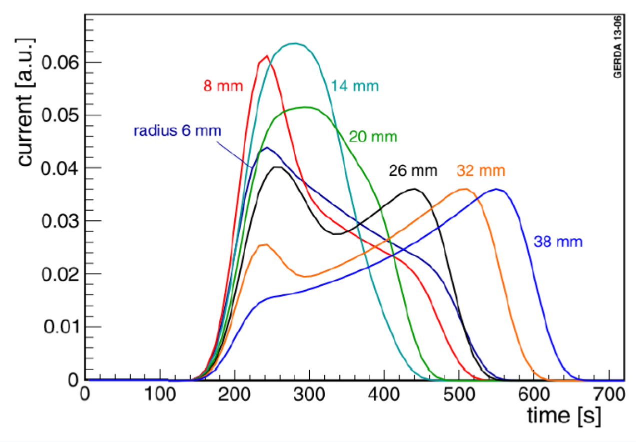

Cut based on ANN using rising part of charge pulse
(tuned using DEP, 2νββ, compton edge events)

$\varepsilon_{PSA}=0.90^{+0.05}_{-0.09}$ for SSE

BI (10^{-3} cts/(keV·kg·yr)) after partial unblinding:

	Before PSA	After PSA
Golden:	$18.5^{+2.3}_{-2.2}$	$10.9^{+1.9}_{-1.6}$
Silver:	$63.4^{+18.0}_{-14.3}$	$30.1^{+13.7}_{-9.8}$

In ROI (golden/silver): 5/1 event detected → 3/0 rejected by PSA

Good agreement with alternative PSA methods

Pulse shape analysis in ROI

Data set	Detector	E (keV)	Date	Passed PSA
golden	ANG5	2041.8	Nov 18, 2011 22:52	–
silver	ANG5	2036.9	Jun 23, 2012 23:02	√
golden	RG2	2041.3	Dec 16, 2012 00:09	√
BEGe	GD32B	2036.6	Dec 28, 2012 09:50	–
golden	RG1	2035.5	Jan 29, 2013 03:35	√
golden	ANG3	2037.4	Mar 2, 2013 08:08	–
golden	RG1	2041.7	Apr 27, 2013 22:21	–

Decays

Decay chains

^{238}U chain

Nuclide	mode	$T_{1/2}$	Q-value (keV)	decay product	E_γ (keV)
^{238}U	α	$4.5\cdot10^9$ yr	4270.0	^{234}Th	–
^{234}Th	β	24.1 d	273.0	^{234m}Pa	–
^{234m}Pa	β	1.2 min	2195.0	^{234}U	–
^{234}U	α	$2.5\cdot10^5$ yr	4858.5	^{230}Th	–
^{230}Th	α	$7.5\cdot10^4$ yr	2770.0	^{226}Ra	–
^{226}Ra	α	$1.6\cdot10^3$ yr	4870.6	^{222}Rn	–
^{222}Rn	α	3.8 d	5590.3	^{218}Po	–
^{218}Po	α	3.1 min	6114.7	^{214}Pb	–
^{214}Pb	β	26.8 min	1024.0	^{214}Bi	351.9
^{214}Bi	β	19.9 min	3272.0	^{214}Po	609.3
					768.4
					1120.3
					1238.1
					1764.5
					2204.2
^{214}Po	α	164.3 μs	7833.5	^{210}Pb	–
^{210}Pb	β	22.3 yr	63.5	^{210}Bi	–
^{210}Bi	β	5.0 d	1162.1	^{210}Po	–
^{210}Po	α	138.4 d	5407.5	^{206}Pb	–

^{232}Th chain

Nuclide	mode	$T_{1/2}$	Q-value (keV)	decay product	E_γ (keV)
^{232}Th	α	$1.4\cdot10^{10}$ yr	4082.8	^{228}Ra	–
^{228}Ra	β	5.8 yr	45.9	^{228}Ac	–
^{228}Ac	β	6.2 h	2127.0	^{228}Th	911.2
					969.0
^{228}Th	α	1.9 yr	5520.1	^{224}Ra	–
^{224}Ra	α	3.7 d	5788.9	^{220}Rn	–
^{220}Rn	α	55.6 s	6404.7	^{216}Po	–
^{216}Po	α	0.1 s	6906.5	^{212}Pb	–
^{212}Pb	β	10.6 h	573.8	^{212}Bi	–
^{212}Bi	β /	60.6 min	2254.0 /	^{212}Po /	727.3
	α		6207.1	^{208}Tl	
^{212}Po	α	0.3 μs	8954.1	^{208}Pb	–
^{208}Tl	β	3.1 min	5001.0	^{208}Pb	510.8
					583.2
					860.6
					2614.5

^{42}Ar: β (599 keV, 33 yr) → ^{42}K: β (3525.4 keV, 1524.7 keV photon, 12 h)
^{40}K: β/β$^+$+ec (1311.1/1504.9 keV, 1460.8 keV photon, $1.3\cdot10^9$ yr)
^{60}Co: β (2823.9 keV, 1173.3 keV & 1332.5 keV photon, 5.3 yr)
^{68}Ge: ec (106.0 keV, 270 d) → ^{68}Ga: ec+β$^+$ (2921.1 keV, 1077.4 keV photon, 67.6 min)

Details on Background Models

Alpha models

Golden data set

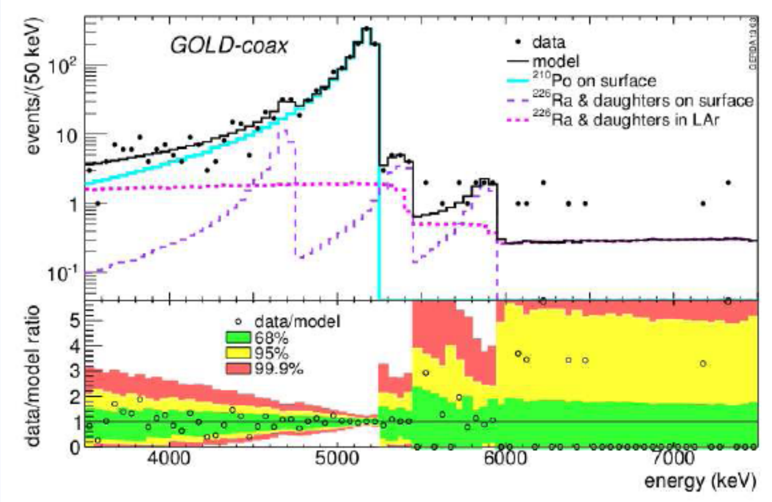

Isotope	Location	Number of counts
^{210}Po	p^+-surface	1355 [1310,1400]
^{226}Ra	p^+-surface	51 [36,65]
^{222}Rn	p^+-surface	25 [18,33]
^{218}Po	p^+-surface	14 [9,19]
^{214}Po	p^+-surface	<10
^{226}Ra	LAr	<159
^{222}Rn	LAr	<64
^{218}Po	LAr	<30
^{214}Po	LAr	20 [10,29]

BEGe data set

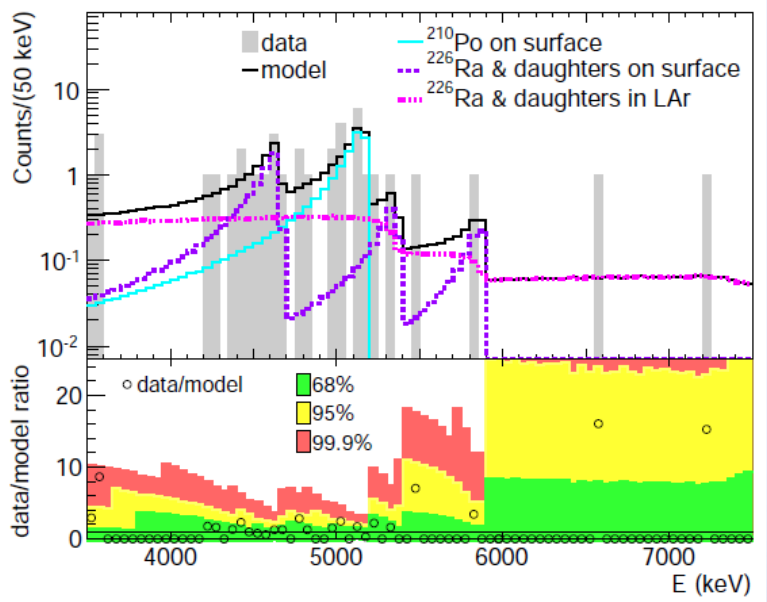

Isotope	Location	Number of counts
^{210}Po	p^+-surface	14.0 [9.4,19.4]
^{226}Ra	p^+-surface	6.1 [2.2,10.2]
^{222}Rn	p^+-surface	<7.1
^{218}Po	p^+-surface	<4.8
^{214}Po	p^+-surface	<4.3
^{226}Ra	LAr	<51.2
^{222}Rn	LAr	<28.6
^{218}Po	LAr	<20.4
^{214}Po	LAr	<12.0

Background model fits golden data

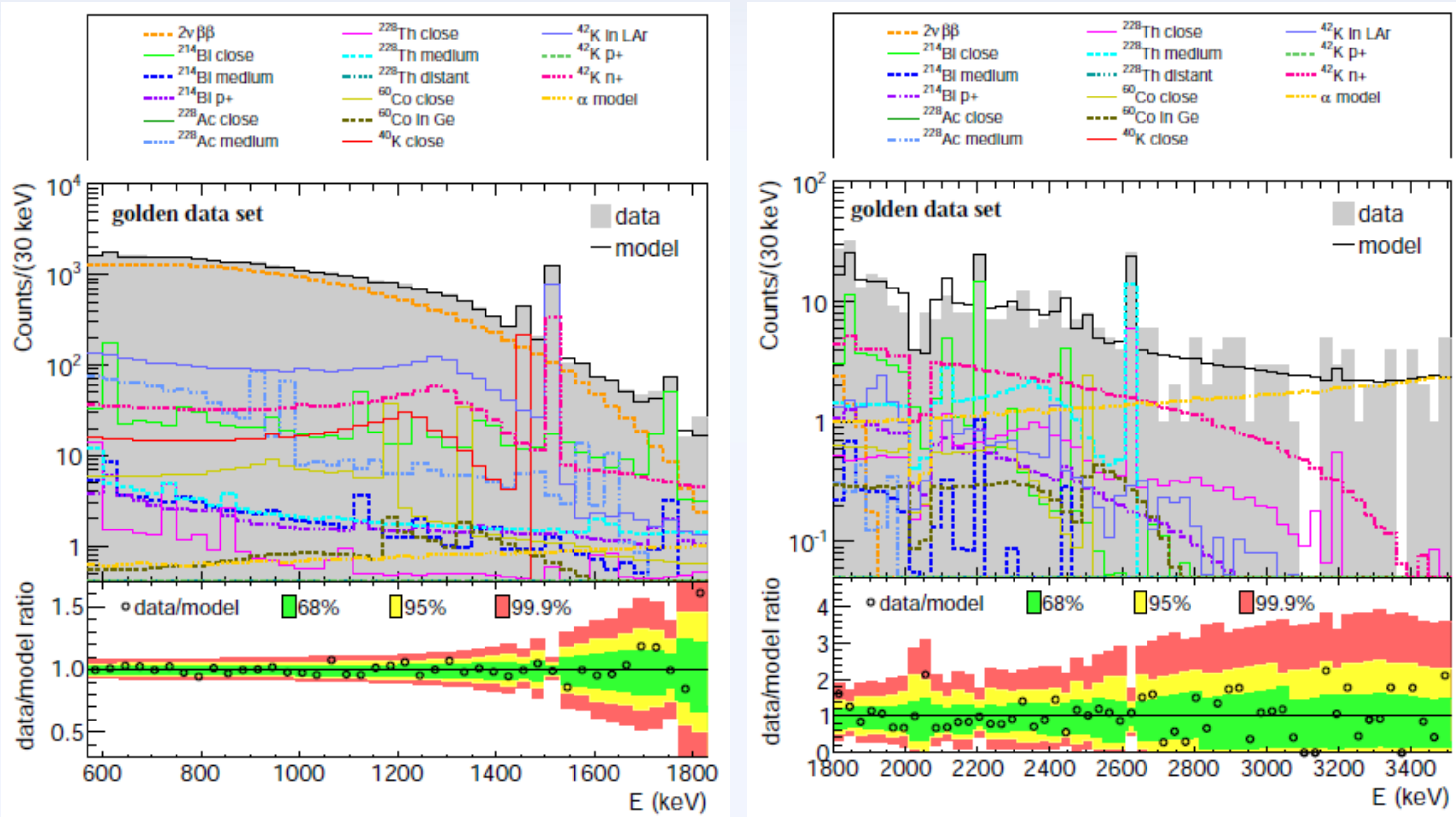

p-value: 0.07

35847 events in data and best-fit model

$T^{2\nu}_{1/2}$=1.94 [1.91,1.97] $\cdot 10^{21}$ yr

Background model around $Q_{\beta\beta}$

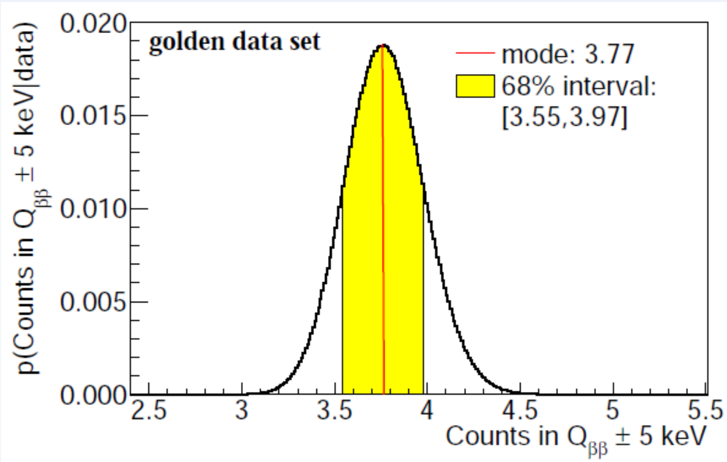

Item	ΔBI_{global}	ΔBI_{marg}	Model composition varied	
			global	marg.
Screening results	–	–	–	–
Active volume fraction				
for internal sources	–	–	–	–
for ^{42}K on n^+-surface	+0.5	+0.4	√	√
Enrichment fraction	–	–	–	–
Source positions	$^{+1.6}_{-0.2}$	$^{+0.2}_{-0.1}$	√	√
Binning	−0.1	−0.1	√	√

Table 9.2: Estimates of the *BI* from the background model in a 10 keV-window around $Q_{\beta\beta}$. Listed are the results for the total model and all individual model components whose spectrum extends up to the window. The global modes, as well as the modes and smallest 68 % interval of the marginalized distributions are given. In case the 68 % interval contains zero, the 90 % quantile of the marginalized distribution is shown. All values are given in units of 10^{-3} cts/(keV · kg · yr).

Isotope	Source position	Global mode	Marg. mode	68 % interval/ 90 % quantile
alpha model	p^+-surface	2.1	2.1	[2.0,2.1]
^{214}Bi chain	close	3.6	2.9	[2.6,3.4]
^{214}Bi chain	medium distant	0.3	0.3	[0.3,1.2]
^{214}Bi chain	p^+-surface	1.3	1.3	[0.9,1.7]
^{228}Th chain	close	1.0	0.8	[0.1,1.4]
^{228}Th chain	medium distant	2.6	0.8	[0.8,2.3]
^{228}Th chain	distant	-		<3.3
^{60}Co	close	1.0	1.0	[0.5,1.5]
^{60}Co	in Ge	0.5		<0.5
^{42}K	LAr	1.7	2.2	[1.9,2.4]
^{42}K	p^+-surface	-		<4.9
^{42}K	n^+-surface	6.2		<5.5
Total		20.3	21.0	[19.8,22.2]

Data (in background window):
$BI = 18.5^{+2.3}_{-2.2} \cdot 10^{-3}$ cts/(keV·kg·yr)

Background model fits BEGe data

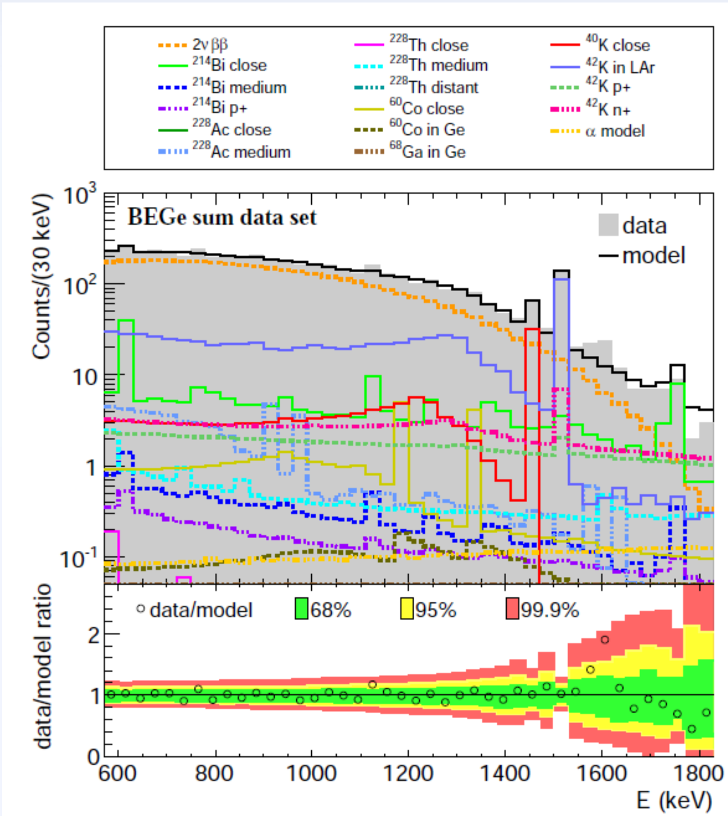

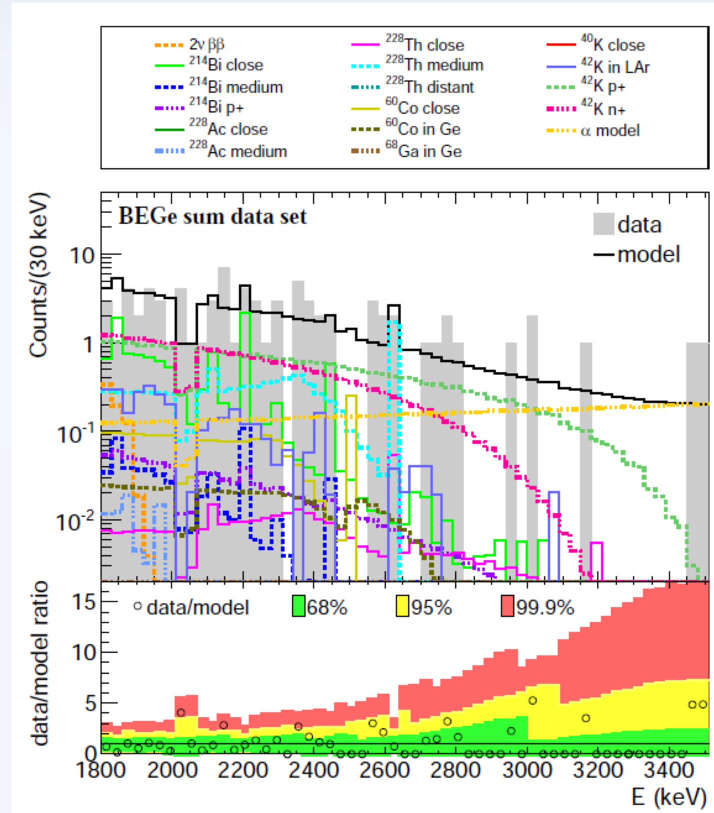

p-value: 0.42
5032 events in data and best-fit model
$T^{2\nu}_{1/2}$=2.10 [2.02,2.19] $\cdot 10^{21}$ yr

Background model around $Q_{\beta\beta}$

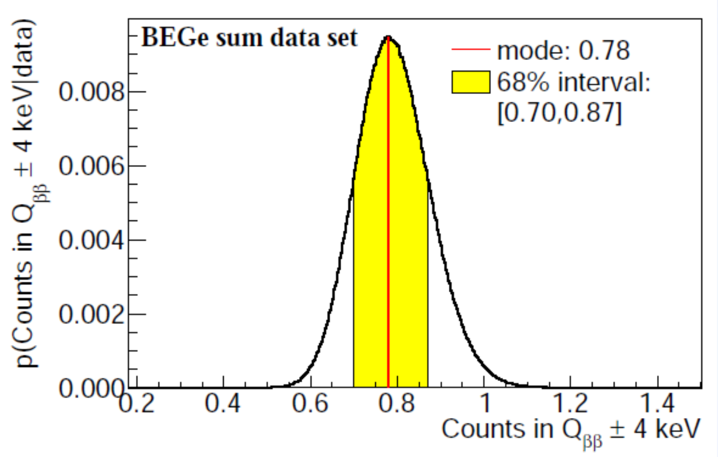

Table 9.5: Estimates of the *BI* from the background model in a 8 keV-window around $Q_{\beta\beta}$. Listed are the results for the total model and all individual model components whose spectrum extends up to the window. The global modes, as well as the modes and smallest 68 % interval of the marginalized distributions are given. In case the 68 % interval contains zero, the 90 % quantile of the marginalized distribution is shown. All values are given in units of 10^{-3} cts/(keV · kg · yr).

Isotope	Source position	Global mode	Marg. mode	68 % interval/ 90 % quantile
alpha model	p^+-surface	1.8	1.8	[1.5,2.1]
^{214}Bi chain	close	5.4	3.2	[2.7,5.1]
^{214}Bi chain	medium distant	0.3	0.3	[0.3,2.7]
^{214}Bi chain	p^+-surface	0.5	0.5	[0.2,0.8]
^{228}Th chain	close	0.1	0.1	[0.1,3.0]
^{228}Th chain	medium distant	3.7	0.8	[0.8,4.2]
^{228}Th chain	distant	-		<8.4
^{60}Co	close	1.2		<4.2
^{60}Co	in Ge	0.3		<0.3
^{68}Ga	in Ge	-		<3.6
^{42}K	LAr	2.0	2.1	[1.9,2.3]
^{42}K	p^+-surface	11.8	5.1	[0.5,10.5]
^{42}K	n^+-surface	12.9		<16.4
Total		40.0	40.6	[36.5,45.2]

Item	ΔBI_{global}	ΔBI_{marg}	Model composition varied global	Model composition varied marg.
Screening results	–	–	–	√
Active volume fraction				
for internal sources	–	+0.3	–	√
for ^{42}K on n^+-surface	−0.4	+0.5	√	√
Enrichment fraction	–	–	–	√
Source positions	$^{+1.1}_{-0.5}$	+1.1	√	√
Binning	$^{+1.3}_{-0.5}$	$^{+1.3}_{-1.2}$	√	√

Data (in background window):
$BI=41.3^{+10.4}_{-8.4}\cdot10^{-3}$ cts/(keV·kg·yr)

Background model prior knowledge

Prior information for single background components:

- ^{214}Bi on p^{+}-surface gaussian prior derived from ^{226}Ra activity determined with alpha model

- ^{60}Co in germanium and ^{68}Ga flat prior with maximum number of events deduced from activation calculations

- Flat prior with minimum number of events for ^{214}Bi on holders and shroud and ^{228}Th on holders and shroud derived from screening measurements

- All remaining background components: Flat priors without restrictions

Component	units	^{40}K	^{214}Bi/^{226}Ra	^{228}Th	^{60}Co	^{222}Rn	BI
Close sources: up to 2 cm from detectors							
Copper det. support	μBq/det	<7	<1.3	<1.5			<0.2
PTFE det. support	μBq/det	6.0 (11)	0.25 (9)	0.31 (14)			0.1
PTFE in array	μBq/det	6.5 (16)	0.9 (2)				0.1
mini-shroud	μBq/det		22 (7)				2.8
Li salt	mBq/kg		17 (5)				≈ 0.003
Medium distance sources: 2 cm to 50 cm from detectors							
CC2 preamps	μBq/det	600 (100)	95 (9)	50 (8)			0.8
cables and suspension	mBq/m	1.40 (25)	0.4 (2)	0.9 (2)	76 (16)		0.2
Distant sources: further than 50 cm from detectors							
cryostat	mBq					54.7 (35)	<0.7
copper of cryostat	mBq	<784	264 (80)	216 (80)	288 (72)		<0.05
steel of cryostat	kBq	<72	<30	<30	475		
lock system	mBq					2.4 (3)	<0.03
^{228}Th calib. source	kBq		20				<1.0

Details on Majoron Analysis

Majoron results

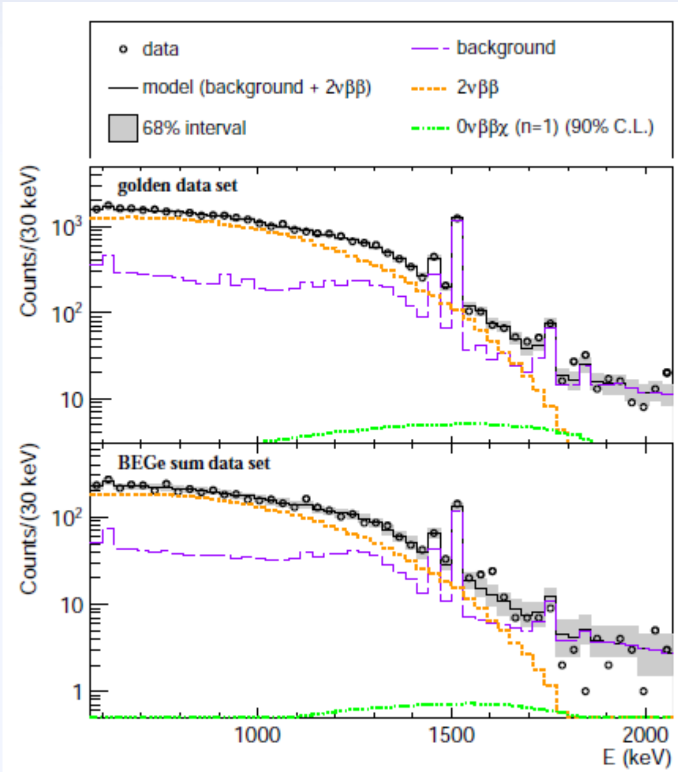

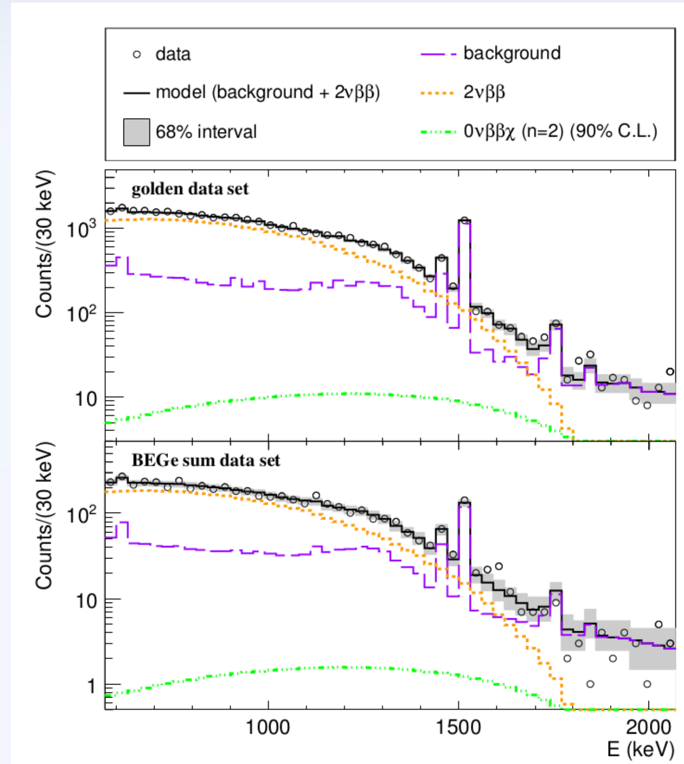

Data: 35868 events in golden, 5035 events in BEGe sum data set

n=1: p-value=0.13
35834.0/5081.4 events
54.5/7.8 Majoron
$T^{2\nu}_{1/2}=1.96\cdot10^{21}$ yr

n=2: p-value=0.14
35794.7/5061.8 events
234.0/33.6 Majoron
$T^{2\nu}_{1/2}=1.97\cdot10^{21}$ yr

Majoron results

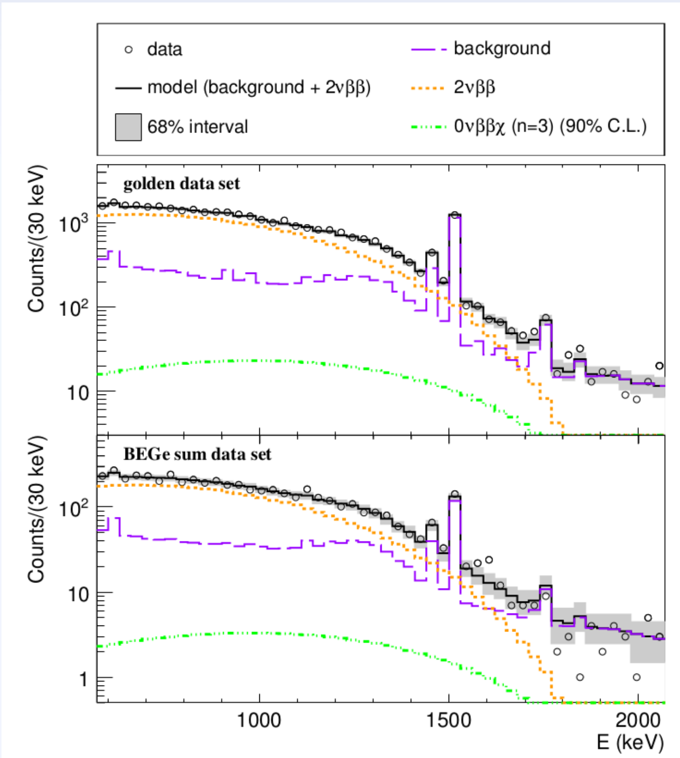

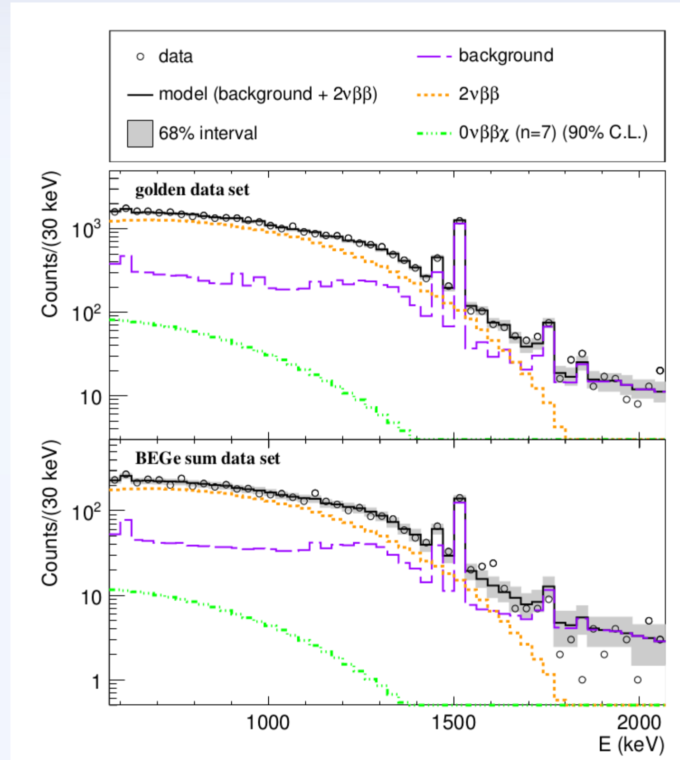

Data: 35868 events in golden, 5035 events in BEGe sum data set

n=3: p-value=0.12
35841.5/5046.4 events
384.9/55.1 Majoron
$T^{2\nu}_{1/2}=1.98\cdot10^{21}$ yr

n=7: p-value=0.13
35795.8/5049.6 events
9.7/1.4 Majoron
$T^{2\nu}_{1/2}=1.99\cdot10^{21}$ yr

Previous results

Half-life $T_{1/2}^{0\nu\chi(\chi)}$ (10^{23} yr)

	This analysis	KamLAND-Zen[1)]	EXO-200[2)]	HdM[3)]
n=1	>4.2	> 26	> 12	> 0.64
n=2	> 1.8	> 10	> 2.5	-
n=3	> 0.8	> 4.5	> 0.27	>0.14
n=7	> 0.3	> 0.11	> 0.06	>0.07

1) *A. Gando et al., Phys. Rev. C 86 (2012)*
2) Phys. Rev. D 90 (2014), 092004
3) *H. V. Klapdor-Kleingrothaus et al., Eur. Phys. J. A 12 (2001), M. Günther, et al., Phys. Rev. D 54 (1996), 3641–3644*

Previous results

Coupling constant $|\langle g_\alpha \rangle|$

	This analysis	KamLAND-Zen[1)]	EXO-200[2)]	HdM[3)]
n=1, χ (IB, IC, IIB)	$< (3.4\text{-}8.7)\cdot 10^{-5}$	$< (0.8\text{-}1.6)\cdot 10^{-5}$	$< (0.8\text{-}1.7)\cdot 10^{-5}$	$< 8.1\cdot 10^{-5}$
n=3, χχ (ID, IE, IID)	$< 2.1^{+4.5}_{-1.4}$	< 0.68	< (0.6-5.5)	< 3.3
n=3, χ (IIC, IIF)	< 0.047	< 0.013	< 0.06	< 0.12
n=7, χχ (IIE)	$< 2.2^{+4.9}_{-1.4}$	< 1.2	< (0.5-4.7)	< 3.3

1) *A. Gando et al., Phys. Rev. C 86 (2012))*
2) Phys. Rev. D 90 (2014), 092004
3) *H. V. Klapdor-Kleingrothaus et al., Eur. Phys. J. A 12 (2001), M. Günther, et al., Phys. Rev. D 54 (1996), 3641–3644*

Sterile Neutrinos

Sterile neutrinos

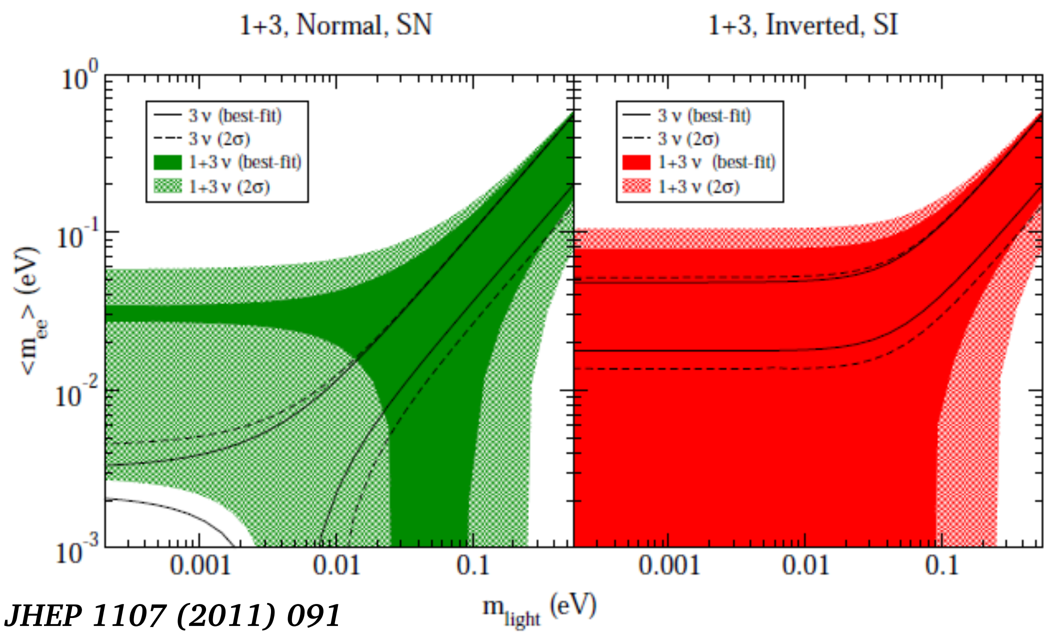

JHEP 1107 (2011) 091

Case of one additional sterile neutrino with $m_{st} >> m_{1,2,3}$:

- $<m_{\beta\beta}> = <m_{\beta\beta}>^{act} + <m_{\beta\beta}>^{st}$
- If $m_{light} < 0.01$ eV → $<m_{\beta\beta}>$ cannot vanish for NH
- $<m_{\beta\beta}>$ can vanish for IH also for small active neutrino masses

References for Phase Spaces and Matrix Elements

References G and M

$G^{0\nu}$:

J. Kotila and F. Iachello, Phase space factors for double-β decay, Phys. Rev. C 85 (2012), 034316

$M^{0\nu}$ & $M^{0\nu\chi}$ (n=1):

- F. Šimkovic, V. Rodin, A. Faessler, and P. Vogel, Phys. Rev. C 87 (2013), 045501
- M. T. Mustonen and J. Engel, Phys. Rev. C 87 (2013), 064302
- T. R. Rodriguez and G. Martinez-Pinedo, Phys. Rev. Lett. 105 (2010), 252503
- J. Menéndez, A. Poves, E. Caurier, and F. Nowacki, Nucl. Phys. A 818 (2009), 139–151
- J. Barea, J. Kotila, and F. Iachello, Phys. Rev. C 87 (2013), 014315
- J. Suhonen and O. Civitarese, Nucl. Phys. A 847 (2010), 207 – 232
- A. Meroni, S. Petcov, and F. Šimkovic, J. High Energy Phys. 2013 (2013), 1–29

$G^{0\nu\chi}$ (n=1) :

J. Suhonen and O. Civitarese, Phys. Rep. 300 (1998), 123 – 214

$G^{0\nu\chi(\chi)}$ & $M^{0\nu\chi(\chi)}$ (n=2, 3, 7) :

M. Hirsch, H. Klapdor-Kleingrothaus, S. Kovalenko, and H. Päs, Phys. Lett. B 372 (1996), 8–14